NASA TECHNICAL NOTE

NASA TN D-5806

NASA TN D-5806

# FLIGHT COMPARISON OF SEVERAL TECHNIQUES FOR DETERMINING THE MINIMUM FLYING SPEED FOR A LARGE, SUBSONIC JET TRANSPORT

*by David A. Kier*

*Flight Research Center*
*Edwards, Calif.* 93523

NATIONAL AERONAUTICS AND SPACE ADMINISTRATION • WASHINGTON, D. C. • JUNE 1970

| 1. Report No. NASA TN D-5806 | 2. Government Accession No. | 3. Recipient's Catalog No. |
|---|---|---|
| 4. Title and Subtitle<br>FLIGHT COMPARISON OF SEVERAL TECHNIQUES FOR DETERMINING THE MINIMUM FLYING SPEED FOR A LARGE, SUBSONIC JET TRANSPORT | | 5. Report Date<br>June 1970<br>6. Performing Organization Code |
| 7. Author(s)<br>David A. Kier | | 8. Performing Organization Report No.<br>H-590 |
| 9. Performing Organization Name and Address<br>NASA Flight Research Center<br>P. O. Box 273<br>Edwards, California 93523 | | 10. Work Unit No.<br>737-05-00-01-24<br>11. Contract or Grant No.<br>13. Type of Report and Period Covered<br>Technical Note |
| 12. Sponsoring Agency Name and Address<br>National Aeronautics and Space Administration<br>Washington, D. C. 20546 | | 14. Sponsoring Agency Code |
| 15. Supplementary Notes | | |

16. Abstract

A flight investigation was conducted to define the minimum flying speed for a large, subsonic jet transport by using three techniques: (1) the Federal Aviation Regulations (FAR) Part 25 demonstration technique; (2) a flight-path 1-g-break technique; and (3) a constant-rate-of-climb technique. The effect of thrust on minimum speed is analyzed.

Results indicate that the flight-path 1-g-break technique was the best overall technique. The constant-rate-of-climb technique, or minimum level-flight speed, though highly affected by the deceleration dynamics of the maneuver, was found to be an acceptable alternate for the 1-g-break technique. The FAR demonstration technique, when analyzed by two current analysis methods, was found to yield the least conservative results. However, if the analysis were based on actual airplane maximum lift capability, the technique would yield acceptable results.

| 17. Key Words Suggested by Author(s) | 18. Distribution Statement |
|---|---|
| Stall<br>Minimum speed<br>Maximum lift coefficient | Unclassified - Unlimited |

| 19. Security Classif. (of this report) | 20. Security Classif. (of this page) | 21. No. of Pages | 22. Price * |
|---|---|---|---|
| Unclassified | Unclassified | 36 | $3.00 |

*For sale by the Clearinghouse for Federal Scientific and Technical Information, Springfield, Virginia 22151.

# FLIGHT COMPARISON OF SEVERAL TECHNIQUES FOR DETERMINING THE MINIMUM FLYING SPEED FOR A LARGE, SUBSONIC JET TRANSPORT

David A. Kier
Flight Research Center

## SUMMARY

A flight investigation was conducted to define the minimum flying speed of a large, subsonic jet transport by using three techniques: (1) the Federal Aviation Regulations (FAR) Part 25 demonstration technique; (2) a flight-path 1-g-break technique; and (3) a constant-rate-of-climb technique. The program consisted of 7 flights for pilot familiarization and 18 flights to obtain data. Approximately 175 stall maneuvers, most in the landing configuration, were performed during the flights.

The 1-g-break technique provided good characteristics at the determined minimum speed in almost all areas investigated, except that determining the 1-g break was complicated by airplane buffeting. The technique yielded a realistic minimum flying speed which was the most conservative, with respect to the maximum lift capability of the airplane, derived by all the techniques investigated.

The constant-rate-of-climb technique, considered only at zero rate of climb for defining the minimum flying speed, provided several good characteristics but was highly influenced by the dynamics of the stall maneuver. Therefore, the minimum speed derived by this technique was not as conservative as the 1-g-break speed, but this technique should be considered as an alternate for the 1-g-break technique.

The FAR technique yielded the least conservative results of the techniques used, but, by modifying the analysis methods, realistic results could be obtained for aircraft having a well-defined maximum lift coefficient.

## INTRODUCTION

The minimum flying speed of an aircraft strongly influences the takeoff, climb, approach, and landing speeds, which, in turn, determine payload capability and runway requirements. For example, the certified approach speed, i.e., the reference speed, for commercial air transports is equal to 1.3 times the minimum flying speed at a given gross weight. The runway landing distance length requirements are based on a reference-speed approach. Reference 1 discusses the specific interrelations of the minimum flying speed with these other factors for the United States Federal Aviation Administration certification of civil air transports. Thus, the determination of an adequate and realistic minimum flying speed is paramount.

During the past decade, the definition of the minimum flying speed for subsonic jet transports has been the subject of considerable controversy. This definition has been dealt with in numerous reports and papers from organizations covering the spectrum of aviation—regulatory agencies (for example, the Federal Aviation Administration), industry, airline pilots, the military, and the National Aeronautics and Space Administration (refs. 1 to 10). Most of these documents agree that the current certification procedures used in determining the minimum speed for civil aviation are fully adequate for straight-wing aircraft, are of questionable adequacy, at best, for aircraft with moderately swept wings, and are wholly inadequate for aircraft with highly swept and delta wings.

The minimum flying speeds for civil air transports are currently defined and determined by Part 25 of the Federal Aviation Regulations (ref. 1). The speed determined by the Regulations (paragraph 25.49) is the "...calibrated stalling speed, or the minimum steady speed, in knots, at which the airplane is controllable, with the...[configuration variables, etc.]." In addition (from paragraph 25.201), "...Typical indications of a stall are a nose-down pitch, or a roll, that cannot be readily arrested, or, if clear enough, a loss of control effectiveness, an abrupt change in control force or motion, characteristic buffeting, or a distinctive vibration of the pilot's controls..."

To investigate the problems of low-speed flight, two flight investigations were made at the NASA Flight Research Center. The first study (ref. 2), conducted on a large, subsonic jet, was a limited overview of the low-speed stability and control characteristics for this type of airplane. This study also briefly investigated minimum speed. The second study (ref. 3), conducted primarily on a small, delta-wing supersonic fighter and briefly on a small, executive jet transport, evaluated the current FAR technique and two alternate techniques for determining the minimum velocity. One of the alternate techniques was based on the ability to maintain a constant 1-g normal acceleration while decreasing speed; the other was based on the ability to maintain a constant rate of climb while decelerating. Since this study was primarily concerned with a small, delta-wing supersonic fighter, the results are not necessarily applicable to large, swept-wing, subsonic transports. The results from the small, executive jet transport study were too meager for any strong conclusions to be drawn.

This report expands the information presented in references 2 and 3. It presents the results of a flight study performed at the NASA Flight Research Center to define the minimum flying speed for a large, subsonic jet transport in the landing configuration. Current certification criteria are evaluated, as well as the two alternate techniques mentioned previously. An analysis of the influence of thrust effects on the determination of the minimum flying speed is included.

## SYMBOLS

| | |
|---|---|
| $a_{n_{ba}}$ | body-axis normal acceleration, g |
| $a_{n_{fp}}$ | flight-path normal acceleration, g |

| | |
|---|---|
| $C_L$ | lift coefficient based on $\frac{Wa_{n_{fp}}}{\bar{q}S}$ |
| $C'_L$ | lift coefficient based on $\frac{W}{\bar{q}S}$ |
| $\Delta C'_L$ | incremental change in lift coefficient |
| $C_{L_{max}}$ | maximum lift coefficient based on $C_L$ |
| $C'_{L_{max}}$ | maximum lift coefficient based on $C'_L$ |
| $C_{L_q}$ | change in lift coefficient with varying pitching velocity without an $\alpha$ change, $\frac{\partial C_L}{\partial\left(\frac{q\bar{c}}{2u}\right)}$ |
| $C_{L_u}$ | change in lift coefficient with variation in forward velocity, $\frac{u}{2}\frac{\partial C_L}{\partial u}$ |
| $C_{L_{\dot{\alpha}}}$ | change in lift coefficient with variation in rate of change of $\alpha$, $\frac{\partial C_L}{\partial\left(\frac{\dot{\alpha}\bar{c}}{2u}\right)}$ |
| $\bar{c}$ | mean aerodynamic chord, ft (m) |
| g | acceleration of gravity, 32.2 ft/sec$^2$ (9.80 m/sec$^2$) |
| h | pressure altitude, ft (m) |
| $\dot{h}$ | time rate of change in altitude or rate of climb, ft/min (m/sec) |
| L/D | lift-to-drag ratio |
| M | Mach number |
| p | static pressure, lb/ft$^2$ (N/m$^2$) |
| q | pitching angular velocity, deg/sec |
| $\bar{q}$ | dynamic pressure, $0.7M^2p$, lb/ft$^2$ (N/m$^2$) |
| S | wing area, ft$^2$ (m$^2$) |

| | |
|---|---|
| $T/W$ | thrust-to-weight ratio |
| $t$ | time, sec |
| $\Delta t$ | time difference, sec |
| $u$ | forward true airspeed, ft/sec (m/sec) |
| $\dot{V}$ | time rate of change of airspeed, $\frac{dV_c}{dt}$, knots/sec |
| $V_c$ | calibrated airspeed, knots |
| $V_g$ | calibrated airspeed at 1-g break, knots |
| $V_{\dot{h}}$ | calibrated airspeed at $\dot{h}$-break, knots |
| $V_{min}$ | minimum calibrated airspeed, knots |
| $V_s$ | FAR stall speed, knots |
| $\Delta V$ | incremental change in the minimum airspeed due to a change in the thrust-to-weight ratio, knots |
| $W$ | airplane gross weight, lb (kg) |
| $\alpha$ | corrected angle of attack referenced to fuselage centerline, deg |
| $\dot{\alpha}$ | time rate of change of $\alpha$, deg/sec |
| $\delta_e$ | elevator position, deg |
| $\rho_o$ | standard atmospheric density at sea level, $2.38 \times 10^{-3}$, slugs/ft$^3$ (1.23 kg/m$^3$) |

Superscript:

| | |
|---|---|
| * | values at maximum lift coefficient |

## DESCRIPTION OF TEST AIRPLANE

The test airplane was a swept-wing jet transport powered by four turbojet, axial-flow, aft-fan engines with a takeoff rating of 16,000 pounds (71,168 newtons) thrust per engine. The wings were equipped with full-span, leading-edge Krueger flaps; partial-span, double-slotted Fowler trailing-edge flaps; and ailerons and spoilers for lateral control. They were swept back 39° at the leading edge, were of a full cantilevered

construction with four antishock bodies, and had an aspect ratio of 6.2. The empennage consisted of a fixed vertical stabilizer with a rudder for directional control, a movable horizontal stabilizer for longitudinal trim, and elevators for longitudinal control. A three-view drawing of the airplane is shown in figure 1, and pertinent physical dimensions are listed in table 1.

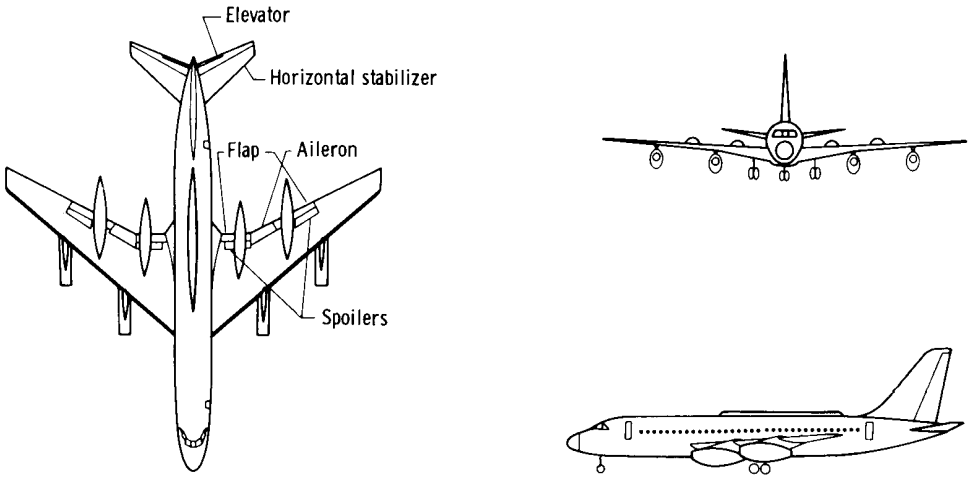


*Figure 1. Three-view drawing of test airplane (test noseboom not shown).*

During normal operation, the primary flight control system of the test airplane was actuated by a combination of mechanical and hydraulic systems. Longitudinal control was normally achieved by using the horizontal stabilizer for trimming and the elevator for maneuvering. The horizontal stabilizer was hydraulically powered and had an electrical and a mechanical backup system. The elevator system was of the reversible, mechanical type. In this system, motion of the control column in the cockpit was transferred by mechanical linkages to a flight tab on the trailing edge of the elevator. This flight tab used aerodynamic forces to move the elevator in a servoed manner; that is, for a nose-up input the flight tab moved down and the elevator moved up.

Lateral control was achieved by using a combination of ailerons and spoilers. The ailerons were powered by a reversible, mechanical system similar to the elevator system. The spoilers were hydraulically powered and were also used as speed brakes.

Directional control was achieved through the rudder by means of a hydraulically powered irreversible system which had a mechanical backup similar to that of the elevator system.

The secondary flight controls (Krueger flaps, Fowler flaps, and landing gear) were hydraulically powered with electrical or mechanical backup systems.

TABLE 1. – PHYSICAL CHARACTERISTICS OF THE TEST AIRPLANE

| | |
|---|---|
| Overall dimensions – | |
| Span, ft (m) | 120 (36.6) |
| Length (nose to trailing edge of elevator panels), ft (m) | 139.20 (42.46) |
| Height (over vertical stabilizer), ft (m) | 39.36 (12.0) |
| Fuselage – | |
| Maximum width (outside), ft (m) | 11.50 (3.51) |
| Cabin interior width, ft (m) | 10.67 (3.25) |
| Maximum height (not including antenna housing), ft (m) | 12.42 (3.79) |
| Length, ft (m) | 134.75 (41.1) |
| Wing – | |
| Airfoil section: | |
| Root (extended chord) | NACA 0011-64 (Mod) |
| 31.5-percent semispan (break) | NACA 0009-64 (Mod) |
| Tip | NACA 0008-64 (Mod) |
| Incidence (root), deg | 4 |
| Span (aerodynamic), ft (m) | 117.99 (35.1) |
| Area (total), $ft^2$ ($m^2$) | 2250 (209.25) |
| Root chord, ft (m) | 29.15 (8.89) |
| Tip chord, ft (m) | 8.83 (2.69) |
| Mean aerodynamic chord (leading edge at fuselage station 821.1 in. (20.86 m)), ft (m) | 20.83 (6.35) |
| Dihedral (at manufacturing chord plane), deg | 7 |
| Aspect ratio, $\frac{Span^2}{Area}$ | 6.2 |
| Sweep (leading edge), deg | 39 |
| Flaps | Double slotted |
| Leading-edge devices (Krueger flaps) | Extensible |
| Engine pod clearance, ft (m): | |
| Inboard | 3.29 (1.00) |
| Outboard | 4.23 (1.29) |
| Horizontal stabilizer – | |
| Airfoil section designation: | |
| Root | NACA 009-64 (Mod) |
| Tip | NACA 008-64 (Mod) |
| Area, $ft^2$ ($m^2$) | 426.5 (27.43) |
| Dihedral, deg | 7.5 |
| Sweep (leading edge), deg | 41 |
| Span, ft (m) | 38.74 (11.81) |
| Vertical stabilizer – | |
| Airfoil section designation: | |
| Root | NACA 0010-64 (Mod) |
| Tip | NACA 0008-64 (Mod) |
| Area, $ft^2$ ($m^2$) | 295 (27.44) |
| Sweep (30-percent chord), deg | 35 |
| Engine – | |
| Type | Aft-fan turbojet with reverser |
| Number | 4 |
| Thrust (each) | 16,000-lb (71,168-N) class |

## INSTRUMENTATION AND DISPLAYS

The test airplane had complete stability and control instrumentation. An airspeed head similar to a NACA standard airspeed head and angle-of-attack and angle-of-sideslip vanes were positioned on a 12-foot (3.66-meter) nose boom. The angle of attack was measured relative to the fuselage reference line and was corrected for airplane pitching angular velocity (ref. 11) and vane upwash (ref. 12).

Data were recorded onboard the airplane on three 26-channel oscillographs and were correlated with 0.1-second timing marks. The resolution and accuracies of several pertinent parameters at approximately test conditions were as follows:

| Parameter | Resolution | Accuracy |
|---|---|---|
| Airspeed, knots | 0.2 | ±0.50 |
| Altitude, ft (m) | 15 (4.58) | ±45 (13.73) |
| Flight-path normal acceleration, g | .003 | ±.01 |
| Flight-path longitudinal acceleration, g | .001 | ±.005 |
| Angle of attack (system), deg | .1 | ±.25 |
| Engine pressure ratio | .01 | ±.02 |

Airplane gross weight and center-of-gravity measurements were obtained from readings taken in flight from the fuel quantity gages on the flight engineer's console. The accuracy of these parameters was: gross weight, approximately ±3000 pounds (±1359 kilograms); and center of gravity, approximately ±1 percent $\bar{c}$.

An airspeed calibration was made on this installation; therefore, all airspeed data are presented in terms of calibrated airspeed. The lag characteristics of the airspeed and altitude systems were established in comprehensive laboratory tests; thus, all data presented are corrected for lag. The lag in the static source was approximately 0.6 second at an altitude of 20,000 feet (6100 meters).

A flight-path accelerometer system was operating in the test airplane during flight. The system consisted of a platform on which a longitudinal accelerometer and a normal accelerometer were mounted. The platform was stabilized along the flight path of the airplane by servoing it to the angle-of-attack-vane position transmitter. The system was corrected for vane upwash and aircraft pitching velocity. The platform position accuracy was better than 1 percent of full scale. The total system accuracy for the normal acceleration was slightly better than 2 percent of full scale, and the system accuracy of the longitudinal accelerometer was approximately 2.4 percent of full scale. The effects of the flight-path accelerometer and a body-axis accelerometer on the results obtained from maneuvers using the 1-g-break technique are discussed in appendix A.

Cockpit displays used in performing the test maneuvers included airspeed, altitude, rate of climb, static free-air temperature, artificial horizon, and engine parameter information. However, several additional parameters were displayed to facilitate the tests; these were angle of attack, angle of sideslip, flight-path normal acceleration, and flight-path longitudinal acceleration. The angles of attack and sideslip were obtained from noseboom flow-direction vanes, and the two accelerations from the flight-path accelerometer system.

## TEST PROCEDURE

The evaluation consisted of 7 pilot familiarization flights and 18 data-acquisition flights, during which approximately 175 stall maneuvers were performed. The maneuvers were divided into three groups: one for the FAR demonstration technique, another for the 1-g-break technique, and the final group for the constant-rate-of-climb technique. The maneuvers are described in detail in the next section. Most of the maneuvers were performed in the landing configuration, i.e., full 50° flaps and landing gear down, and were initiated between altitudes of 14,000 feet (4270 meters) and 18,000 feet (5490 meters) in order to minimize Reynolds number effects. The maneuvers were performed over a gross-weight range of 130,000 pounds (58,890 kilograms) to 215,000 pounds (97,395 kilograms), the most readily available range for the test airplane. This weight range corresponded to a wing-loading variation of approximately 58 $lb/ft^2$ (2777 $N/m^2$) to 96 $lb/ft^2$ (4596 $N/m^2$). The center-of-gravity variation was restricted to 23 percent to 26 percent $\bar{c}$, which corresponded to a mid-center-of-gravity variation for the airplane.

Pilot comments were tape recorded after each maneuver or series of maneuvers. Comments were solicited in the following four areas:

1. Longitudinal characteristics - pitchup tendency, adequate control power, and control forces.

2. Lateral-directional characteristics - rolloff tendency or other stability problems, adequate control power, and control forces.

3. Piloting skill - any special pilot skill or technique required either in maneuver or recovery not mentioned in items 1 or 2.

4. Other relevant comments.

The rationale used in evaluating the techniques was that the minimum speed should be conservative (safe), repeatable, and realistic; consistent in determining the maximum usable lift capability of the aircraft—with or without thrust; and reasonably easy to demonstrate, not requiring any unusual piloting skill. In addition, the technique should be applicable to all types of aircraft.

## DESCRIPTION OF THE MANEUVERS

### FAR Demonstration Technique

The maneuvers used in the FAR demonstration technique were initiated from a straight-flight, trim condition at 130 percent of the certified stall speed ($1.3\,V_S$) for the test gross-weight condition. The throttles were set to meet the test power requirements; unless otherwise noted, this setting was outboard engines at idle and inboard engines at 82-percent rpm (82-percent rpm setting on the inboard engines was used to reduce cabin pressurization transients). This power setting yielded a thrust-to-weight ratio of less than 0.02. The airplane was then decelerated without changing any of

the trimming devices.

During the maneuver, the task was to fly a constant deceleration while maintaining a steady, wings-level attitude until the airplane exhibited the stall characteristics of (from ref. 1, paragraph 25.201) "...nose-down pitch, or a roll, that cannot be readily arrested, or, if clear enough, a loss of control effectiveness, an abrupt change in control force or motion, characteristic buffeting, or a distinctive vibration of the pilot's controls..." Operating under these constraints, the pilots usually terminated the maneuver when the angle of attack was 25° to 30°, which is well above the contractor's predicted value at stall of 13° to 14°. (Limited manufacturer's aerodynamic predictions for the test airplane were available.) The maneuvers were never terminated because of lateral-directional problems alone. However, the lateral-directional handling was degraded at the higher angles of attack and required more than normal pilot attention, which did contribute to the pilots' decisions to discontinue a large percentage of the maneuvers.

### 1-g-Break Technique

The 1-g-break technique was initiated from the $1.3V_S$ trim point, as were the FAR maneuvers. Again, trim was not changed during the maneuver and the throttles were at the settings used in the FAR maneuvers. For this technique, however, the task was to fly a constant 1-g flight-path normal acceleration while decreasing speed. The pilot decelerated the airplane until he could no longer maintain a 1-g flight condition and then continued the deceleration until the nose of the airplane dropped, or until the other stall characteristics mentioned previously became apparent.

### Constant-Rate-of-Climb Technique

The constant-rate-of-climb technique was also initiated from a $1.3V_S$ trim point, with trim and power settings the same as for the FAR demonstration and 1-g-break maneuvers. For this technique, the task was to fly a constant rate of climb or descent while decelerating. The pilot continued the maneuver beyond the point at which the constant rate of climb was lost, until the nose of the airplane dropped or other stall manifestations appeared.

## RESULTS AND DISCUSSION

### FAR Stall Speed Demonstration Technique

The calibrated stall speed or minimum steady flight speed defined by the Federal Aviation Regulation for current subsonic civil aircraft is determined at a deceleration $\dot{V}$ of 1 knot/second or less. Although the Regulations define a flight demonstration technique, they do not specify data-analysis methods or restrictions on the maneuver other than the rate of change of airspeed. Therefore, the FAR maneuvers will be analyzed by using two current methods, the $C_L'$ method and the $\dot{V}$ versus $V_{min}$ method.

$C'_L$ analysis method. – In the $C'_L$ method a $C'_{L_{max}}$ is calculated from the flight data and $C'_L$ is corrected for a deceleration equal to 1 knot per second. The $C'_L$ at 1 knot/second is then converted to airspeed at the test gross weight. The $C'_L$ parameter differs from the conventional $C_L$ parameter in that the calculation of $C'_L$ does not include normal acceleration. An example of the application of this analysis method follows.

A time history of the last 28 seconds of a typical FAR stall maneuver for the test airplane in the landing configuration (flaps 50°, gear down) is shown in figure 2(a). For the $C'_L$ analysis method, the only parameters of interest are the test gross weight, initial trim altitude, minimum airspeed obtained, and rate of change of airspeed. Therefore, in figure 2(a) only the airspeed trace is of direct interest. Near $t = 20$ seconds, the slope of the airspeed trace changes, producing a "bucket" just prior to reaching its minimum value. This bucket complicates the determination of the deceleration, since the question arises of which rate of change of airspeed to use—before the slope change or after the slope change.

The policy set forth in the Civil Aeronautics Manual 4b - Airplane Airworthiness: Transport Categories (replaced by FAR Part 25) is still used in determining $\dot{V}$; namely, the slope of a straight line drawn from 110 percent of the minimum speed to the minimum speed is the deceleration. In figure 2(a), the $\dot{V}$ obtained by this method is approximately -1.4 knots/second.

Once $\dot{V}$ has been determined, the next step in this analysis method is to calculate $C'_{L_{max}}$ by using the following equation:

$$C'_{L_{max}} = \frac{W_{test}}{\bar{q}S} \tag{1}$$

Since $W$ is assumed to be constant during the maneuver, $C'_{L_{max}}$ will maximize where $\bar{q}$ is minimized; this, of course, occurs at the minimum velocity. Then $C'_{L_{max}}$ is plotted against $\dot{V}$. Figure 2(b) presents the results from 18 stall maneuvers on the test airplane using the FAR flight demonstration technique and the $C'_L$ analysis method.

The $C'_{L_{max}}$ for each data point is then corrected for the effects of the deceleration by calculating $\Delta C'_L$ due to the deceleration using the following equation:

$$\Delta C'_L = \frac{1}{(\text{Slope})}(-1 - \dot{V}) \tag{2}$$

where the slope is the slope of the faired line in figure 2(b). The reference deceleration, as seen from equation (2), is 1 knot/second.

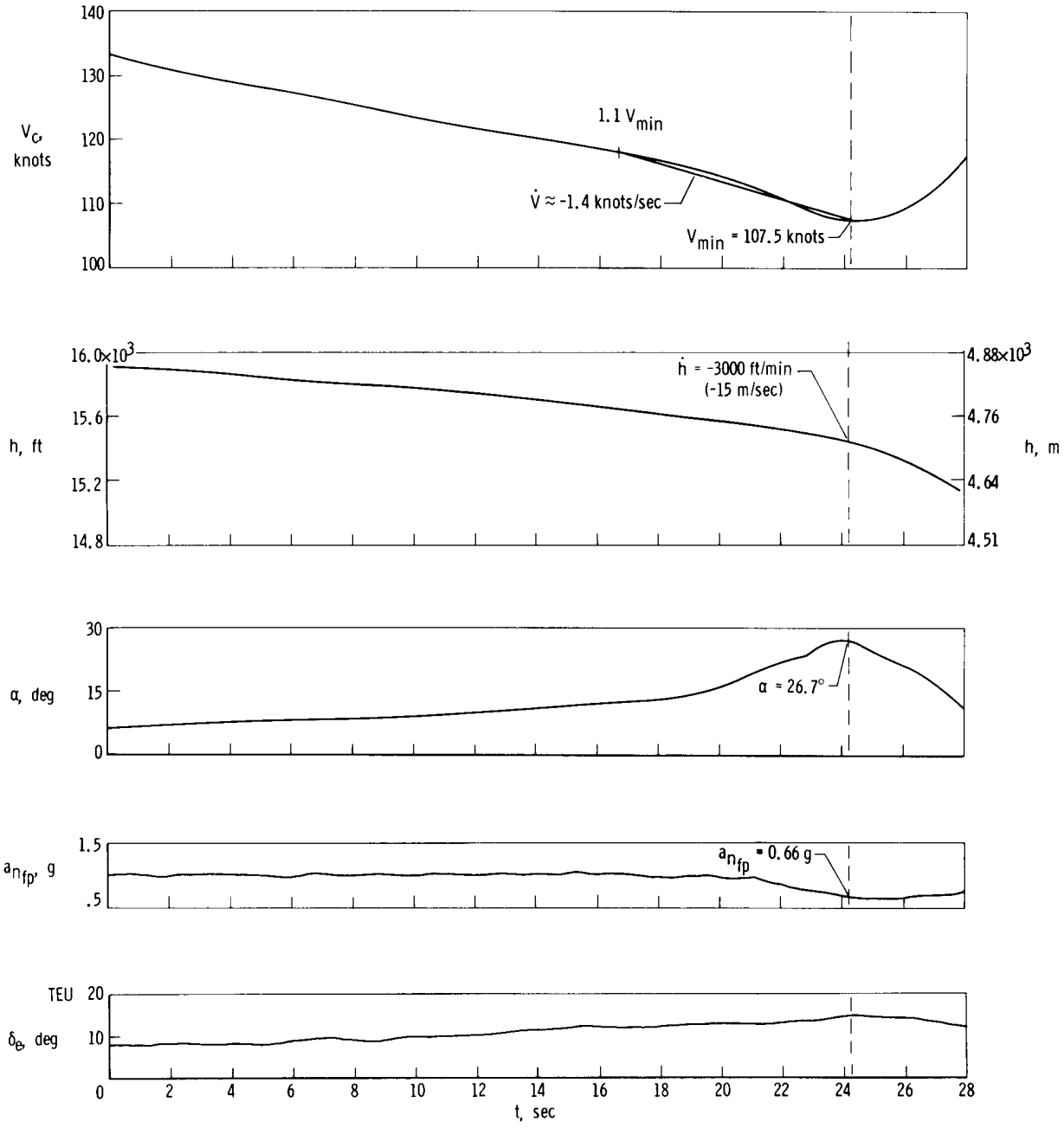


*(a) Typical time history of a FAR stall maneuver; W = 162,500 lb (73,613 kg); center of gravity = 24 percent $\bar{c}$.*

*Figure 2. Analysis of FAR stall-demonstration-technique maneuvers performed in the landing configuration.*

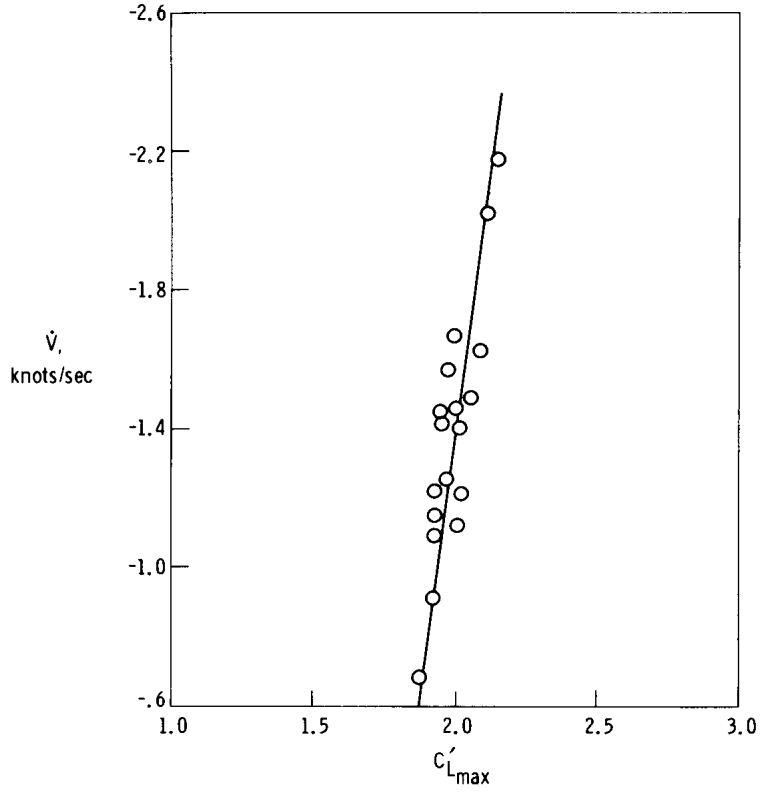


*(b) Correction of $C'_L$ analysis method data to $\dot{V}$ = -1 knot/sec; W = 156,000 lb (70,668 kg) to 168,000 lb (76,104 kg); center of gravity = 23.5 percent to 26 percent $\bar{c}$; h = 13,800 ft (4209 m) to 17,800 ft (5429 m).*

*Figure 2. Continued.*

The test gross weight of the airplane for the maneuvers of figure 2(b) varied from 156,000 pounds (70,668 kilograms) to 168,000 pounds (76,104 kilograms). Since the gross weight is of prime importance in the calculation of $C'_{L_{max}}$, it is recommended that the weight variation in the maneuvers to be used in this type of analysis not exceed 10 percent of the total test weight of the airplane. Thus, several plots of the type in figure 2(b) would be necessary to cover the operational gross-weight range of a large transport. The large gross-weight variation can affect $C'_{L_{max}}$ in two ways: aeroelasticity and a slight effect on $\dot{V}$. Neither effect is large, but in combination they can account for approximately a 2-percent variation in $C'_{L_{max}}$ from light to heavy gross-weight conditions.

To proceed from $C'_{L_{max}}$ at $\dot{V}$ = -1 knot/second obtained from figure 2(b) to the stall speed at $\dot{V}$ = -1 knot/second, the following equations are used:

$$\left.\begin{aligned} u &= \sqrt{\frac{2W}{\rho_o C'_{L_{max}} S}} \\ V_s &= \sqrt{0.131 \frac{W}{C'_{L_{max}}}} \end{aligned}\right\} \qquad (3)$$

Figure 2(c) compares the stall speed as determined from the $C_L'$ method for 36 maneuvers over the gross-weight range for the test airplane with the certified stall speed as published in the test airplane's flight manual. The maximum difference between any single flight check point and the certified speed is 2 knots. This difference is attributable to data scatter, different instrumentation and data-acquisition systems, and some slight aircraft configuration differences.

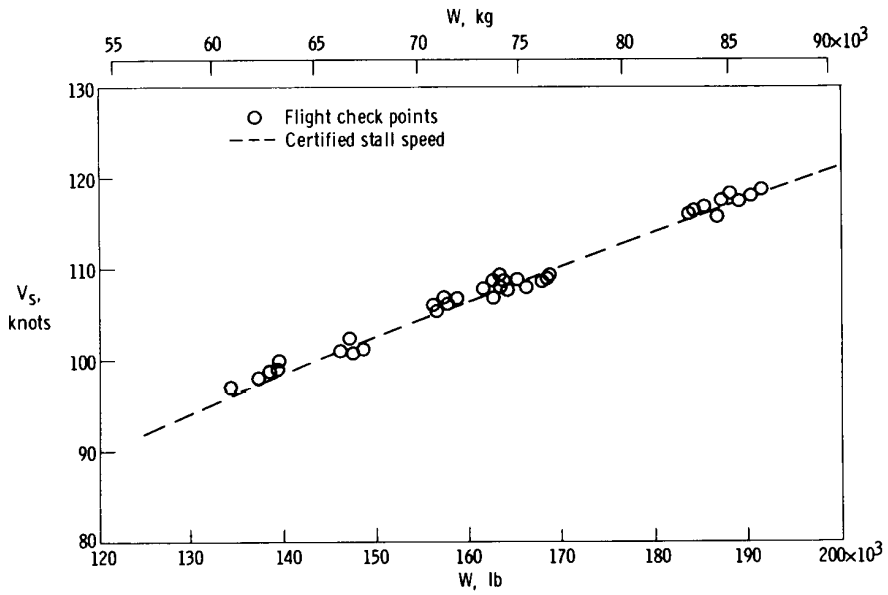


*(c) Comparison of flight check points analyzed by $C_L'$ method with the certified stall speed.*

*Figure 2. Continued.*

$\dot{V}$ versus $V_{min}$ analysis method. – In the second analysis method, $\dot{V}$ versus $V_{min}$, the airspeed is corrected to a constant gross weight, over a limited gross-weight range. Then the deceleration requirement of 1 knot per second is satisfied by plotting $\dot{V}$ against $V_{min}$ and choosing $V_S$ at $\dot{V} = -1$ knot/second. An example of this method follows.

Three quantities are required for the $\dot{V}$ versus $V_{min}$ method: test gross weight, minimum airspeed, and rate of change of airspeed. Referring to the time history of figure 2(a), the only parameter of interest for applying this method is again the airspeed trace. The minimum speed and the rate of change of speed are chosen in the same manner as in the $C_L'$ method. But the $\dot{V}$ versus $V_{min}$ method requires a constant gross weight; therefore, the minimum speed of any particular maneuver must be corrected to a reference gross weight (ref. 11), in this instance, 165,000 pounds (74,745 kilograms). The gross-weight correction to the deceleration is assumed to be

negligible. The gross-weight variation should be less than 10 percent of the test weight to retain assumption validity and to limit the correction factors.

The use of this method on data from the same 18 maneuvers as used with the $C'_L$ method yields the data and variation shown in figure 2(d). Note that a $\dot{V}$ change of 1 knot/second would result in a $V_{min}$ change of approximately 7 knots. Since the

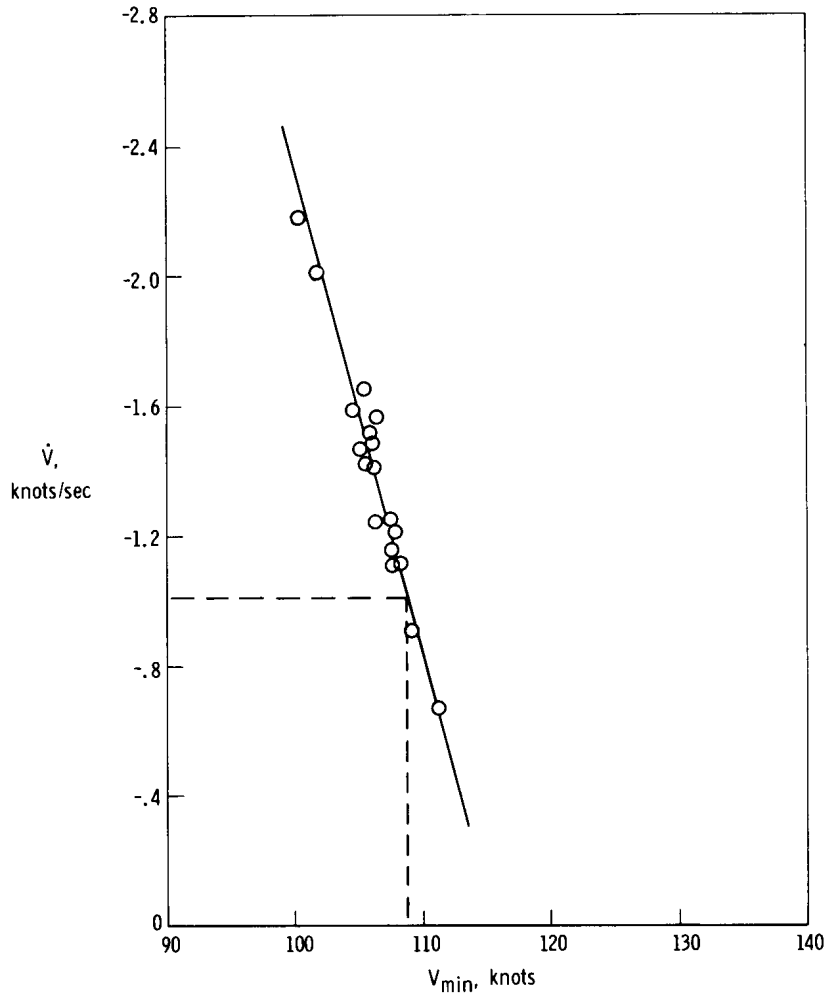


*(d) Correction of the $\dot{V}$ versus $V_{min}$ analysis method data to $\dot{V}$ = -1 knot/sec; $W_{corrected}$ = 165,000 lb (74,745 kg).*

*Figure 2. Continued.*

Regulations specify that the speed reduction should not exceed 1 knot per second, the $V_S$ chosen for this configuration and weight at $\dot{V}$ = -1 knot per second would be 109 knots. In figure 2(e), which presents the rates of climb at which $V_{min}$ was reached for the same 18 stalls as in figure 2(d), the sink rate for 109 knots would be the highly adverse rate of approximately 3300 feet per minute (16.5 meters per second). Also, even at the high deceleration rates (2.0 to 2.2 knots/second), the sink rate is of the order of 800 feet per minute (4 meters per second).

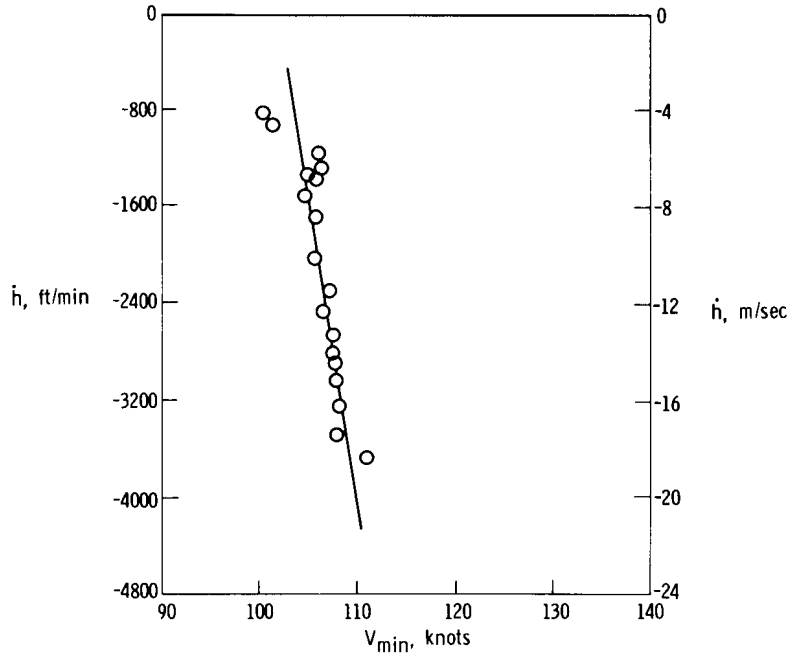


*(e) Rate of climb obtained at $V_{min}$; $W_{corrected}$ = 165,000 lb (74,745 kg).*

*Figure 2. Continued.*

Actual-maximum-lift-coefficient method. – The actual-maximum-lift-coefficient method is similar to the $C'_L$ analyses method except that the actual lift coefficient $C_L$ is used instead of the $C'_L$ coefficient. The method involves calculating the actual maximum lift coefficient from the flight time history, plotting the speed at which $C_{L_{max}}$ occurs against $\dot{V}$, and then using the speed at $\dot{V}$ = -1 knot/second as the defined speed.

The coefficient $C_L$ is calculated from the same parameters as $C'_L$ with $a_{n_{fp}}$ included in the numerator as shown in the following expressions:

$$C'_L = \frac{W}{\bar{q}S}$$

$$C_L = \frac{Wa_{n_{fp}}}{\bar{q}S}$$

Figure 2(f) repeats the time history shown in figure 2(a) with the addition of two parameters, $C'_L$ and $C_L$. As expected, $C'_L$ maximizes where $\bar{q}$, hence $V_c$, is minimized. As shown, $C_L$ maximizes approximately 3 seconds earlier than $C'_L$. Comparing the parameters at the times when $C_L$ and $C'_L$ maximize, it is noted

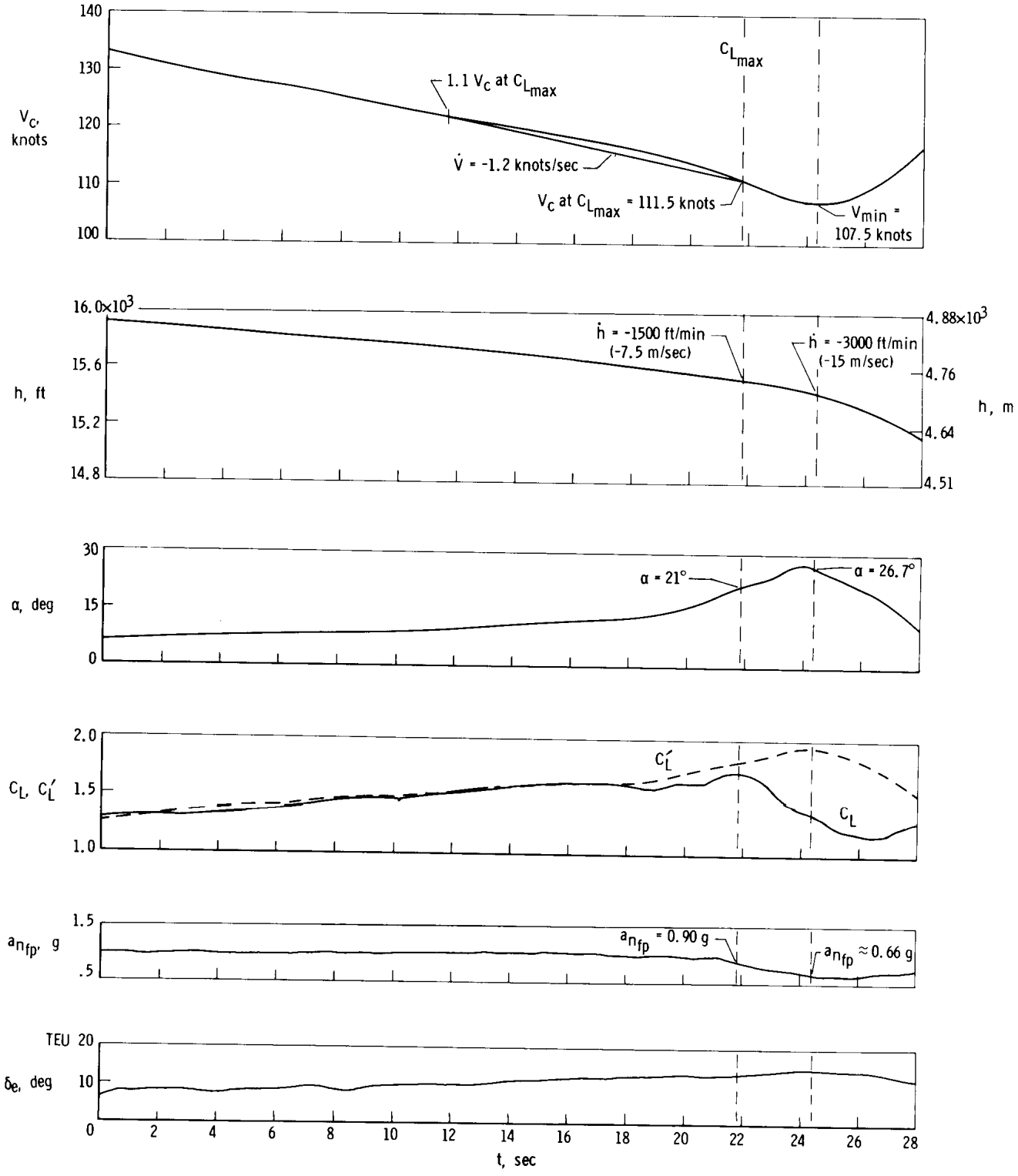


*(f) Time history of FAR stall maneuver illustrating variations of $C_L'$ and $C_L$ during the maneuver; W = 162,500 lb (73,613 kg); center of gravity = 24 percent $\bar{c}$.*

*Figure 2. Continued.*

that: the airspeed at $C_{L_{max}}$ is 111.5 knots compared to 107.5 knots at $C'_{L_{max}}$; the angle of attack is 21° at $C_{L_{max}}$ compared to 26.7° at $C'_{L_{max}}$; the sink rates are 1500 feet per minute (7.5 meters per second) at $C_{L_{max}}$ and 3000 feet per minute (15 meters per second) at $C'_{L_{max}}$; and the $a_{n_{fp}}$ is 0.90 g at $C_{L_{max}}$ and 0.66 g at $C'_{L_{max}}$. This comparison implies that the point at which $C_L$ maximizes yields more conservative results than the point at which $C'_L$ maximizes.

Comparison of $V_{min}$ determined by various analysis methods. – A comparison of the minimum speed determined by the $C'_L$ and $\dot{V}$ versus $V_{min}$ analysis methods, the speed at which $C_L$ maximizes, and the certified stall speed is shown as a variation of gross weight in figure 2(g). Each symbol represents the same 36 FAR stall maneuvers performed on the test airplane but analyzed by the different methods. However, each symbol also represents a speed that has been corrected to the gross weights indicated and that corresponds to a deceleration of 1 knot/second. The minimum speeds determined by the $C'_L$ method and the $\dot{V}$ versus $V_{min}$ method are in excellent agreement, with a maximum difference of approximately 0.5 knot, and also agree well with the certified stall speed, with a maximum difference of approximately 1 knot. This is to be expected because these two methods are virtually equivalent; they use the same data but in slightly different fashion. The minimum speeds determined at $C_{L_{max}}$ are between 4 knots and 5.5 knots greater than the certified stall speed.

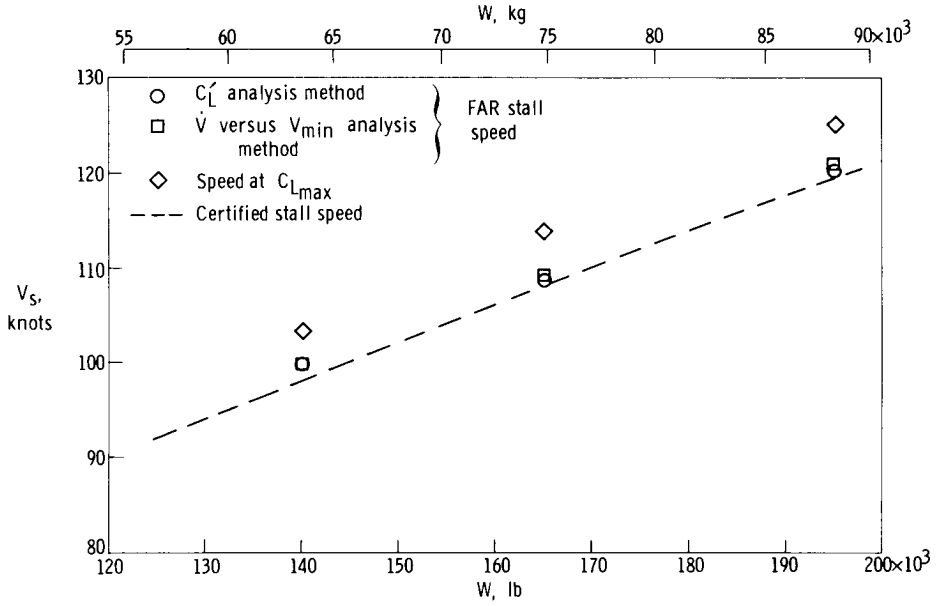


*(g) Comparison of $V_{min}$ obtained from same 36 FAR stall maneuvers analyzed by different methods.*

*Figure 2. Continued.*

Thrust effects. – Six additional stall maneuvers were performed to ascertain the effect of thrust on the stall speed. The thrust-to-weight ratio for these maneuvers was 0.11, which is approximately one-half the maximum T/W available at the test gross-weight condition and is significantly greater than the value of $T/W < 0.02$ used in the other FAR demonstration technique maneuvers. The extra energy or rate of energy expenditure contributed by thrust has two effects. The first is to lower $V_{min}$ at a corresponding $\dot{V}$. Figure 2(h) shows, for example, that at $\dot{V} = -1$ knot/second, the $V_{min}$ is lowered by approximately 2.5 knots. Although $V_{min}$ is lowered, thrust does not greatly influence the effects of the deceleration; that is, a $\dot{V}$ change of 1 knot/second still causes a 6-knot change in $V_{min}$ at this thrust-to-weight ratio.

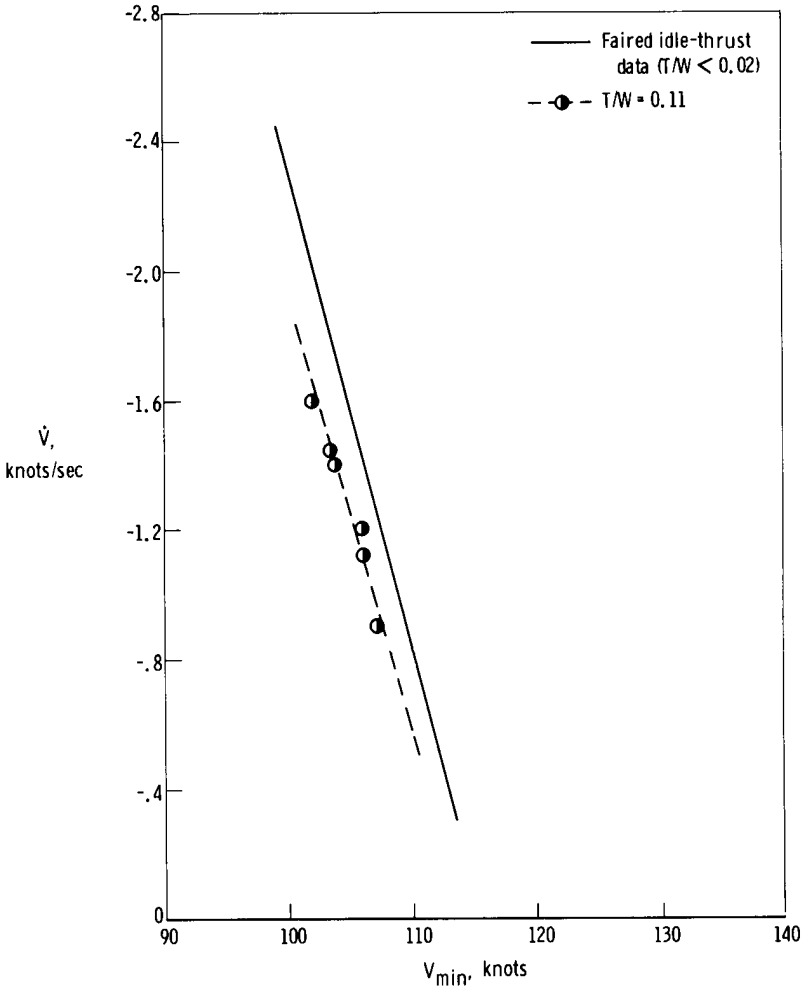


*(h) Thrust effects on $V_{min}$ with varying $\dot{V}$; $W_{corrected}$ = 165,000 lb (74,745 kg).*

*Figure 2. Continued.*

The second effect of the extra energy is to lower the sink rates at $V_{min}$, as shown in figure 2(i).

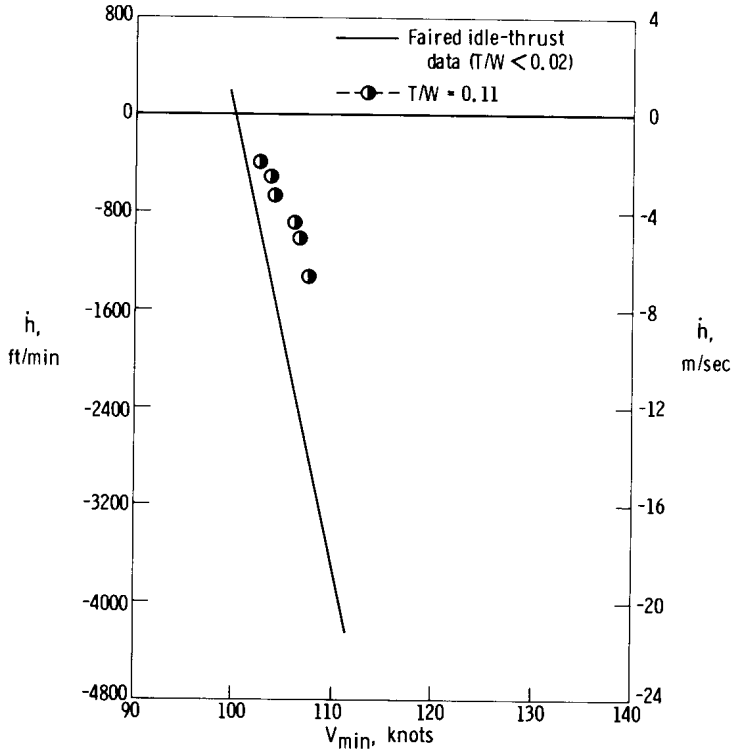


*(i) Thrust effects on rate of climb at $V_{min}$; $W_{corrected}$ = 165,000 lb (74,745 kg).*

*Figure 2. Concluded.*

## 1-g-Break Stall Technique

An alternate for the FAR technique of minimum-speed determination is the 1-g-break technique. This technique defines the minimum speed as that speed below which the airplane can no longer sustain 1-g flight. For this series of tests, the flight-path normal acceleration was used for all calculations of minimum speed and time histories.

Analysis of technique. – A typical time history of the last 28 seconds of a 1-g-break stall maneuver performed on the test airplane in the landing configuration is shown in figure 3(a). Once the 1-g-break point is established (to be discussed later), the minimum speed for this particular maneuver is obtained as shown in the figure. At the 1-g-break, the $a_{n_{fp}}$ is 0.97 g, the angle of attack is 18°, the airspeed is 111.5 knots, and the sink rate is only 220 feet per minute (1.10 meters per second). Shortly after the g breaks (approximately 1.3 seconds), $C_L$ reaches a maximum and the airspeed is approximately 109 knots. Since the g-break occurs before $C_{L_{max}}$ is reached, the 1-g-break-technique speed is considered to be conservative with respect to the speed attained at maximum lift during this maneuver. The deceleration is determined, to be consistent, in the same manner as it was in the FAR maneuvers; that is, by the slope of the straight line from the airspeed at 1-g break to $1.1\,V_g$. For the 1-g-break maneuver illustrated, the airspeed trace is nearly linear up to the 1-g break, with the bucket in the trace occurring after the g-break. This was true for all the 1-g-break maneuvers.

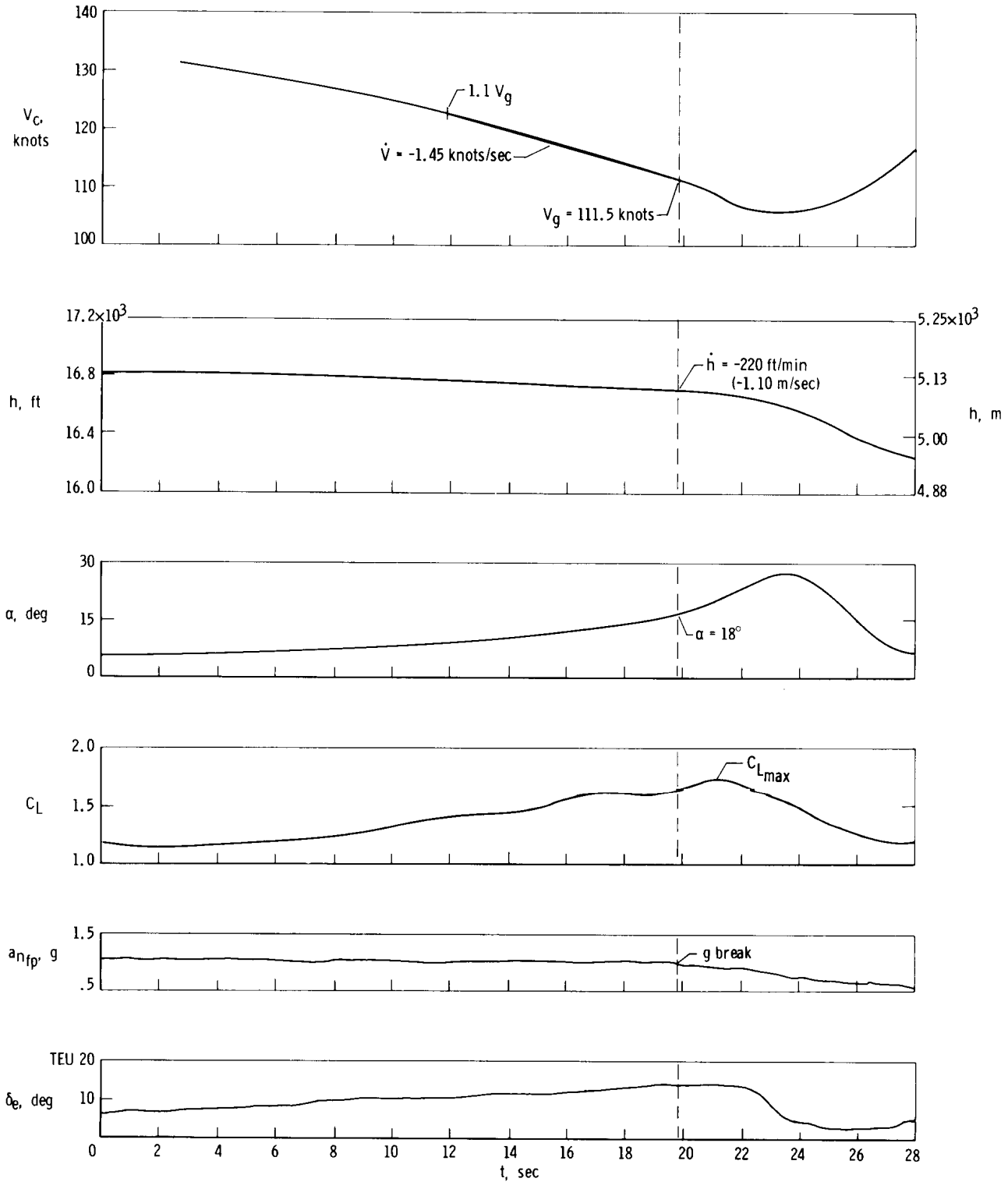


*(a) Typical time history of a 1-g-break stall maneuver; W = 161,500 lb (73,160 kg); center of gravity = 24.1 percent $\bar{c}$.*

*Figure 3. Analysis of 1-g-break stall-technique maneuvers performed in the landing configuration.*

Summary plots for 19 1-g-break stalls are shown in figures 3(b) and 3(c). The value of $V_g$ has been corrected to a speed corresponding to a constant gross weight of 165,000 pounds (74,745 kilograms) (ref. 11). The gross-weight range for these maneuvers was 156,000 pounds (70,668 kilograms) to 169,000 pounds (76,557 kilograms); the maximum difference between the range extremes and 165,000 pounds (74,745 kilograms) was less than 10 percent of 165,000 pounds (74,745 kilograms).

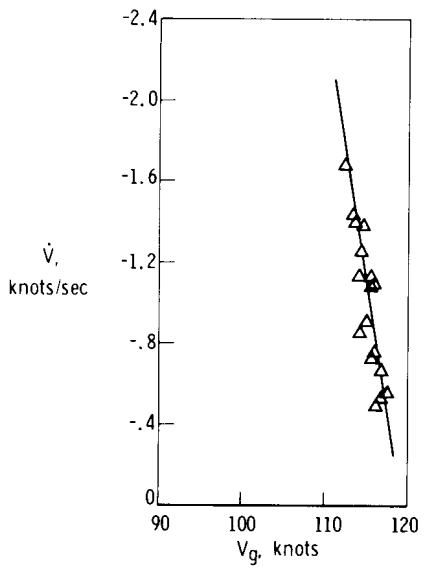


*(b) Effect of $\dot{V}$ on $V_g$ at $W_{corrected}$ = 165,000 lb (74,745 kg).*

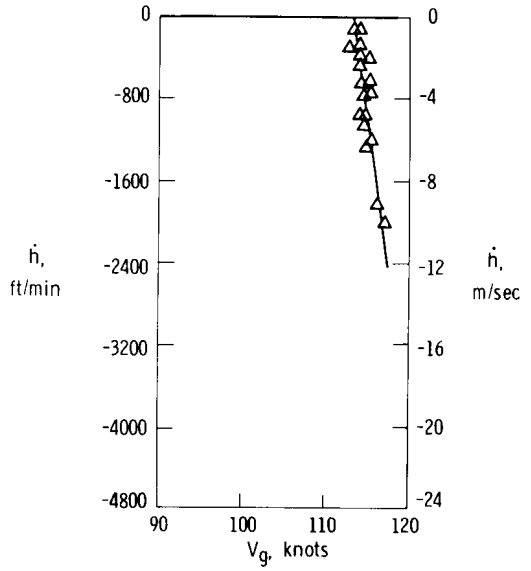


*(c) Rate of climb obtained at $V_g$ for maneuvers of figure 3(b); $W_{corrected}$ = 165,000 lb (74,745 kg).*

*Figure 3. Continued.*

The deceleration dynamics of the maneuver still affect $V_g$ (fig. 3(b)); a $\dot{V}$ change of 1 knot/second corresponds to a $V_g$ change of approximately 3 knots. The FAR maneuvers had a larger $V_{min}$ versus $\dot{V}$ slope, 7 knots/second. At a deceleration of 1 knot/second, $V_g$ is approximately 115 knots, and at 115 knots the corresponding $\dot{h}$ is approximately -800 feet per minute (-4 meters per second) (fig. 3(c)). This sink rate is approximately one-fourth the magnitude of the sink rate for the FAR maneuvers at $\dot{V}$ = -1 knot/second.

Although the 1-g-break technique yields a realistic minimum flying speed with respect to flight conditions and flight characteristics, it has two obvious difficulties. The first is defining the 1-g break. For this series of tests, the 1-g break was defined as that point where an obvious drop in the normal-acceleration level occurred. For example, if the normal-acceleration trace was averaging 0.98 g to 1.02 g for some time as the airplane decelerated, and then suddenly dropped to 0.95 g and continued at this level or lower, the g-break was considered to have occurred. However, if there was no sudden drop in the level of normal acceleration but a gradual drift away from 1 g occurred, the break point was chosen as the point where the normal-acceleration trace fell below 0.97 g, not to be regained. In the study of reference 3 a condition was encountered in which the acceleration fell below the 1-g level and then was regained

for a short period by using large control inputs. This phenomenon could not be duplicated on the test airplane. Once the normal-acceleration level dropped below 0.97 g for longer than 1 second, the pilot could not regain that level, even with the use of very large control inputs.

The process of determining the 1-g-break point was also complicated by airplane buffeting, which caused the acceleration trace to become ragged and discontinuous. This effect was minimized as much as possible by shock-mounting the accelerometer platform and filtering the accelerometer output. Although these measures were relatively effective, data from approximately 5 percent of the maneuvers had to be discarded because the 1-g-break point could not be determined adequately.

A second difficulty with the 1-g-break technique is the necessity of correlating an accelerometer output and a pressure-sensor output, that is, from normal acceleration to airspeed at a specific time. To accomplish this transition accurately, the lags in the airspeed system must be accounted for.

Thrust effects. – The results of test maneuvers made with a thrust-to-weight ratio of 0.11 are shown in figures 3(d) and 3(e). This thrust-to-weight ratio is approximately 50 percent of the highest possible ratio for the test airplane at this weight. The $\dot{V}$ to $V_g$ and the $\dot{h}$ to $V_g$ relationships remained essentially unchanged, with the same slopes as in the idle-thrust runs. The effect of thrust on this technique was, as shown, small.

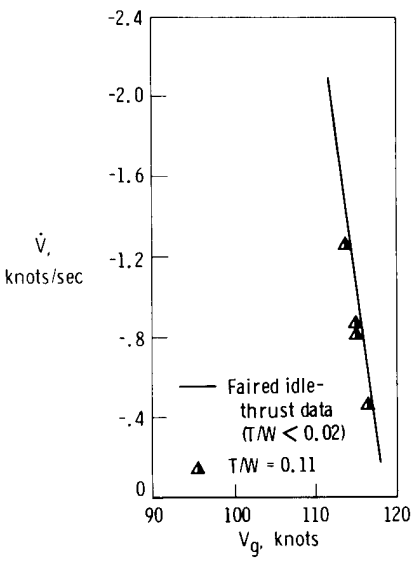


*(d) Thrust effects on $V_g$ with varying $\dot{V}$; $W_{corrected}$ = 165,000 lb (74,745 kg).*

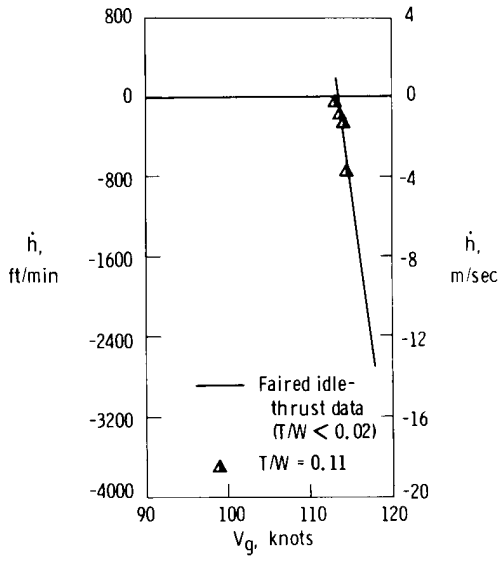


*(e) Thrust effects on rate of climb at $V_g$; $W_{corrected}$ = 165,000 lb (74,745 kg).*

*Figure 3. Concluded.*

## Constant-Rate-of-Climb Stall Technique

The constant-rate-of-climb stall technique, advocated in reference 4 and applied in reference 3, is the second alternate for the FAR minimum-speed technique and

defines the minimum speed as that speed below which a constant rate of climb can no longer be sustained. The climb rates cited herein were determined from the slope of the altitude trace on the test time histories.

Analysis of technique. – A typical time history of the last 28 seconds of a constant-rate-of-climb maneuver performed in the landing configuration is shown in figure 4(a). The altitude trace during this maneuver has a relatively linear characteristic slope until it reaches $t \approx 21$ seconds. At this time, the trace begins to diverge from the constant slope. The point at which the slope begins to diverge is the $\dot{h}$-break, which occurs within the bucket of the velocity trace. When the $\dot{h}$ broke for this maneuver, the rate of climb was -1040 feet per minute (-5.2 meters per second), the angle of attack was 19.4°, and the $a_{n_{fp}}$ was 0.88 g. The deceleration $\dot{V}$ was determined (again for consistency) to be the slope of the straight line from the speed at which $\dot{h}$ breaks ($V_{\dot{h}}$) to 1.1 $V_{\dot{h}}$, as shown in the figure. Also shown is a time history of lift coefficient $C_L$ during the maneuver. The coefficient maximizes approximately 1 second before the $\dot{h}$ breaks, indicating that this technique is slightly nonconservative with respect to the maximum lift capability of the airplane.

A summary of data from the constant-rate-of-climb stalls for a range of $\dot{h}$ corrected to a constant gross weight is presented in figure 4(b). Also shown is the calculated variation of $V_{\dot{h}}$ with $\dot{h}$ based on the equations developed in reference 3. At the lower rates of climb, the slopes of the curves have different polarity, whereas, at the higher sink rates, the polarity of the slopes is similar. Figure 4(c), which shows the variation of $\dot{V}$ with $V_{\dot{h}}$, provides an explanation for this difference. The trend in the data of this figure shows the customary lower $V_{\dot{h}}$ with higher $\dot{V}$ and vice versa. This would indicate that the dynamics as represented by $\dot{V}$ are controlling the maneuver and therefore the $V_{\dot{h}}$ obtained for each stall.

In reference 3 and reference 4 the zero rate of climb is considered to be optimum for use in specifying a minimum flying speed for this technique. Thus, the speed of interest, that at zero rate of climb, is 111.5 knots. The actual $\dot{V}$ for the two points at $\dot{h} = 0$ are -2.3 and -2.4 knots/second, respectively (solid symbols fig. 4(c)). This relatively high value of $\dot{V}$ corresponds to a $V_{\dot{h}}$ about 4 knots lower than at $\dot{V} = -1$ knot/second. The value of $\dot{V}$ obtained during a zero-rate-of-climb maneuver at idle thrust varies greatly with airplane configuration, primarily as a result of differing lift-to-drag ratios[1] at maximum lift coefficient (L/D)*. On the test airplane, for example, in the clean configuration $\dot{V}$ at zero rate of climb is 1.9 to 1.7 knots/second. The (L/D)* for the clean configuration is 12 to 13, whereas in the landing configuration the (L/D)* is between 6 and 7.

During the test program, data from approximately 5 percent of all the constant-rate-of-climb maneuvers had to be discarded as unusable primarily because of (1) the inability to determine an $\dot{h}$ prior to stall, and (2) the inability to select the point at which $\dot{h}$ breaks. The first problem was attributable mainly to piloting technique; that is, if the airplane attitude and $\dot{h}$ were oscillating, the actual approach rate of climb could not

[1]The lift-to-drag ratio was approximated by using the inverse tangent of the flight-path angle.

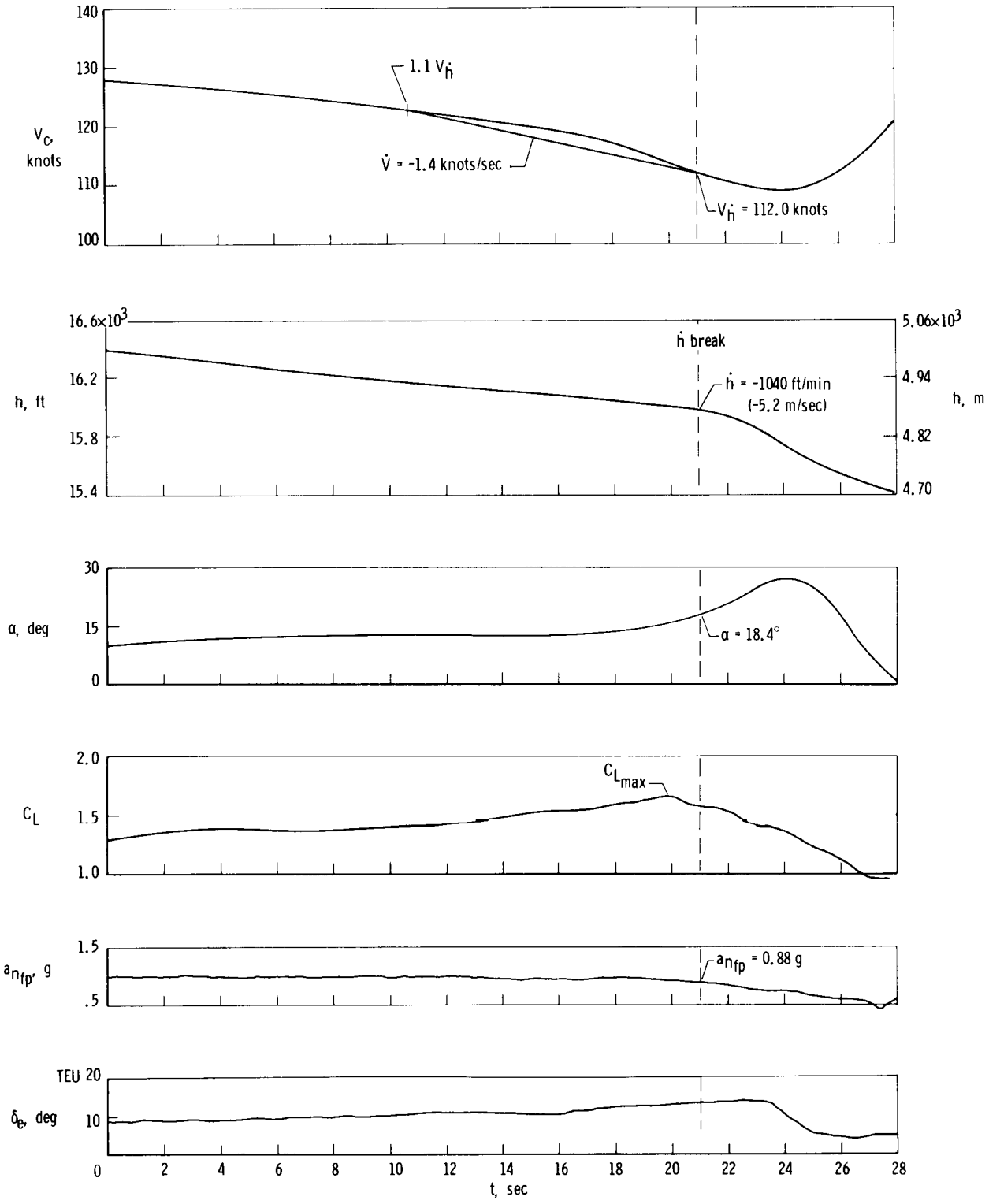


*(a) Typical time history of a constant-rate-of-climb stall maneuver; W = 168,000 lb (76,104 kg); center of gravity = 24.2 percent $\bar{c}$.*

*Figure 4. Analysis of the constant-rate-of-climb stall-technique maneuvers performed in the landing configuration.*

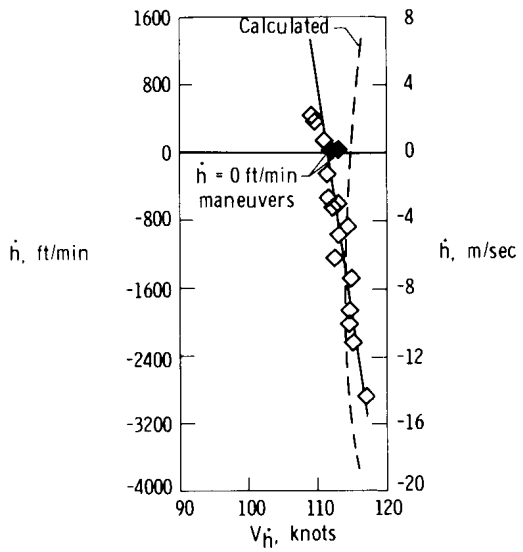


*(b) Rate of climb obtained at $V_{\dot{h}}$; $W_{corrected}$ = 165,000 lb (74,745 kg).*

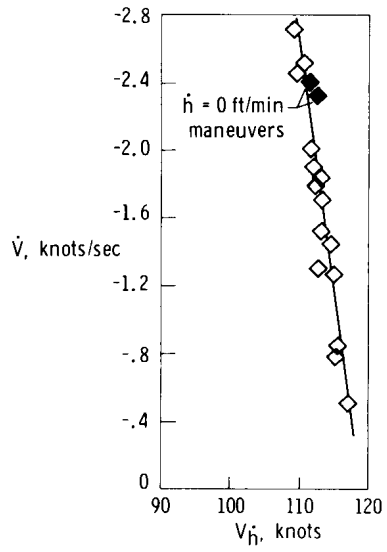


*(c) $\dot{V}$ obtained at $V_{\dot{h}}$ for maneuvers of figure 4(b); $W_{corrected}$ = 165,000 lb (74,745 kg).*

*Figure 4. Continued.*

be determined with sufficient accuracy. The second problem usually, but not always, was a result of the first. The difficulty in determining the $\dot{h}$-break is attributed to sensitivity, resolution, and frequency response of the altitude-sensing instrumentation, and to setting acceptable deviation limits from the target $\dot{h}$ in the maneuver.

Another area of potential difficulty would occur if the static-pressure source for the altitude-measuring system and the airspeed-measuring system had considerably different line lengths or different locations. The lags in each system would be different and thus would have to be evaluated and compensated for during data analysis. This was not a problem on the test airplane, since the static source was common to both systems and the line lengths were within a few inches of one another.

Thrust effects. – Several constant-rate-of-climb stall maneuvers were performed at a thrust-to-weight ratio of 0.11. The resultant data (fig. 4(d)) show that at this ratio the speed at which the zero rate of climb can no longer be maintained is approximately 115.5 knots, which is 4 knots higher than the speed obtained at idle thrust. Thus, adding thrust, up to one-half of that available, actually raised $V_{\dot{h}}$ at zero rate of climb. An explanation of this rather unusual occurrence is shown in figure 4(e). The deceleration for the 0.11 thrust-to-weight-ratio test points is approximately one-half of that for the idle-thrust points at comparable rates of climb. (Compare solid symbols in figs. 4(b) and (c) with comparable test points in figs. 4(d) and (e).) This implies that the dynamics (deceleration, dynamic lift, and inertial effects) of the maneuver, as represented by the deceleration, which is the predominant effect, are more effective than thrust in producing a lower minimum speed up to the level tested, at comparable rates of climb.

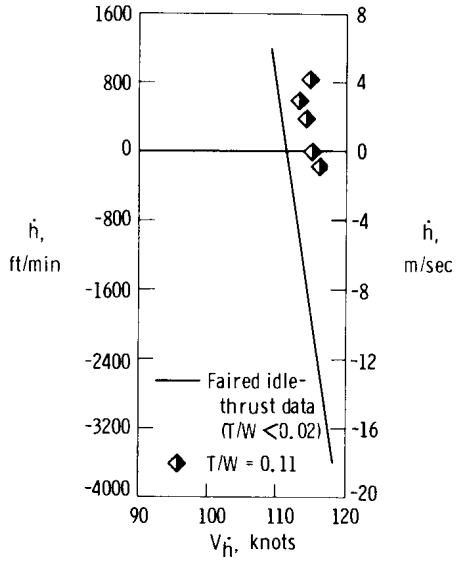


*(d) Thrust effects on $V_{\dot{h}}$ at various values of $\dot{h}$. $W_{corrected}$ = 165,000 lb (74,745 kg).*

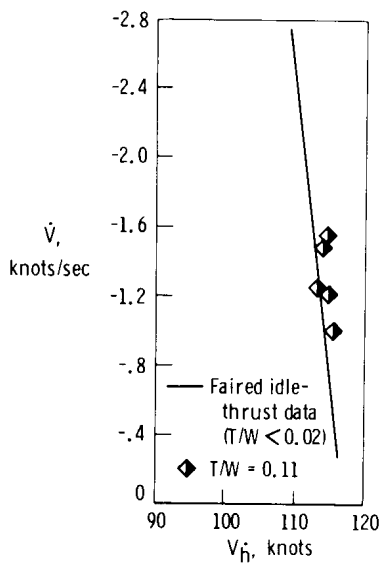


*(e) Thrust effects on $\dot{V}$ at $V_{\dot{h}}$; $W_{corrected}$ = 165,000 lb (74,745 kg).*

*Figure 4. Concluded.*

## Pilot Comments

The pilots felt that some practice was required to perform consistent and repeatable maneuvers, regardless of the technique, but that the maneuvers were not difficult and none required any exceptional piloting skill. Pilot comments indicated that the test airplane had a mild stick-force lightening or a very mild pitchup at high angles of attack and the more aft center-of-gravity locations. When the center of gravity was moved forward by 3-percent $\bar{c}$, the stick-force lightening was alleviated and the pilots could fly the airplane into the stall until the nose dropped. Pilot comments indicated that with the more forward center-of-gravity location the longitudinal response of the airplane to control inputs was generally satisfactory.

Comments concerning the lateral-directional characteristics indicated that this mode was generally satisfactory both in stability and in control response with the yaw damper on; however, it was degraded somewhat at angles of attack above 20°.

The pilots also believed that the higher thrust levels required more attention and effort to yield consistent and repeatable maneuvers. With or without thrust, the pilots had no clear preference for any maneuver or technique but felt that the level-flight (1-g-break or zero-rate-of-climb) maneuvers were the easiest to perform.

## Comparison of Techniques

The minimum flying speeds determined by the three techniques advanced for subsonic jet transport aircraft are compared for three gross weights in figure 5(a). The FAR speed is an average of the speeds determined from the $C_L'$ analysis method and the $\dot{V}$ versus $V_{min}$ analysis method (fig. 2(g)). Also shown is the speed at which

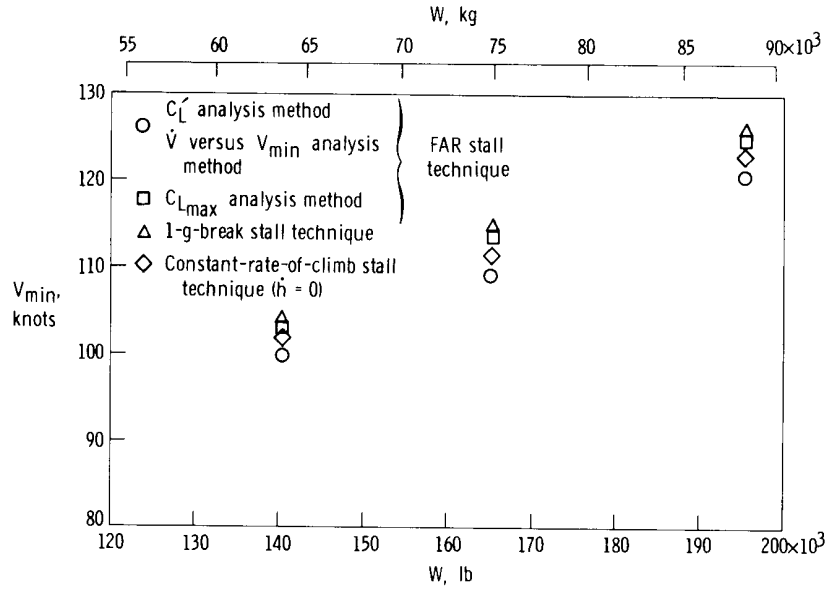


*(a) Comparison of the minimum speeds for three gross weights at $\dot{V}$ = -1 knot/sec or zero rate of climb.*

*Figure 5. Comparison of the three techniques for stall maneuvers performed in the landing configuration; center of gravity = 23.0 percent to 26.3 percent $\bar{c}$; h = 13,600 ft (4148 m) to 18,600 ft (5673 m).*

$C_L$ reached a maximum during the FAR demonstration stalls. Both sets of data derived from the FAR technique are corrected to the gross weights indicated and correspond to $\dot{V}$ = -1 knot/second. The 1-g-break speed corresponds to $\dot{V}$ = -1 knot/second, and it, also, is corrected for gross weight. The constant-rate-of-climb technique is represented by the speed for $\dot{h}$-break at zero rate of climb (corrected for gross weight).

The speeds derived from the FAR technique (by averaging the results from the $C'_L$ method and the $\dot{V}$ versus $V_{min}$ method) yield the lowest airspeeds. The results from the actual-maximum-lift-coefficient method are between 4 knots and 5 knots above these points; the zero-rate-of-climb points are approximately 3 knots greater; and the 1-g points are 5 to 6 knots higher.

Seven parameters, considered to be of primary importance in evaluating a technique for minimum-speed determination, are compared in figure 5(b) at the point at which each technique would establish the minimum flying speed. For example, the constant-rate-of-climb data are at the zero-rate-of-climb break speed and conditions, and the FAR technique data are at the speed corresponding to $\dot{V}$ = -1 knot/second. All data are corrected to 165,000 pounds (74,745 kilograms). The $C_{L_{max}}$ data are treated separately from the other FAR data analyzed by the $C'_L$ method and the $\dot{V}$ versus $V_{min}$ method. The seven parameters are considered individually in the following discussion.

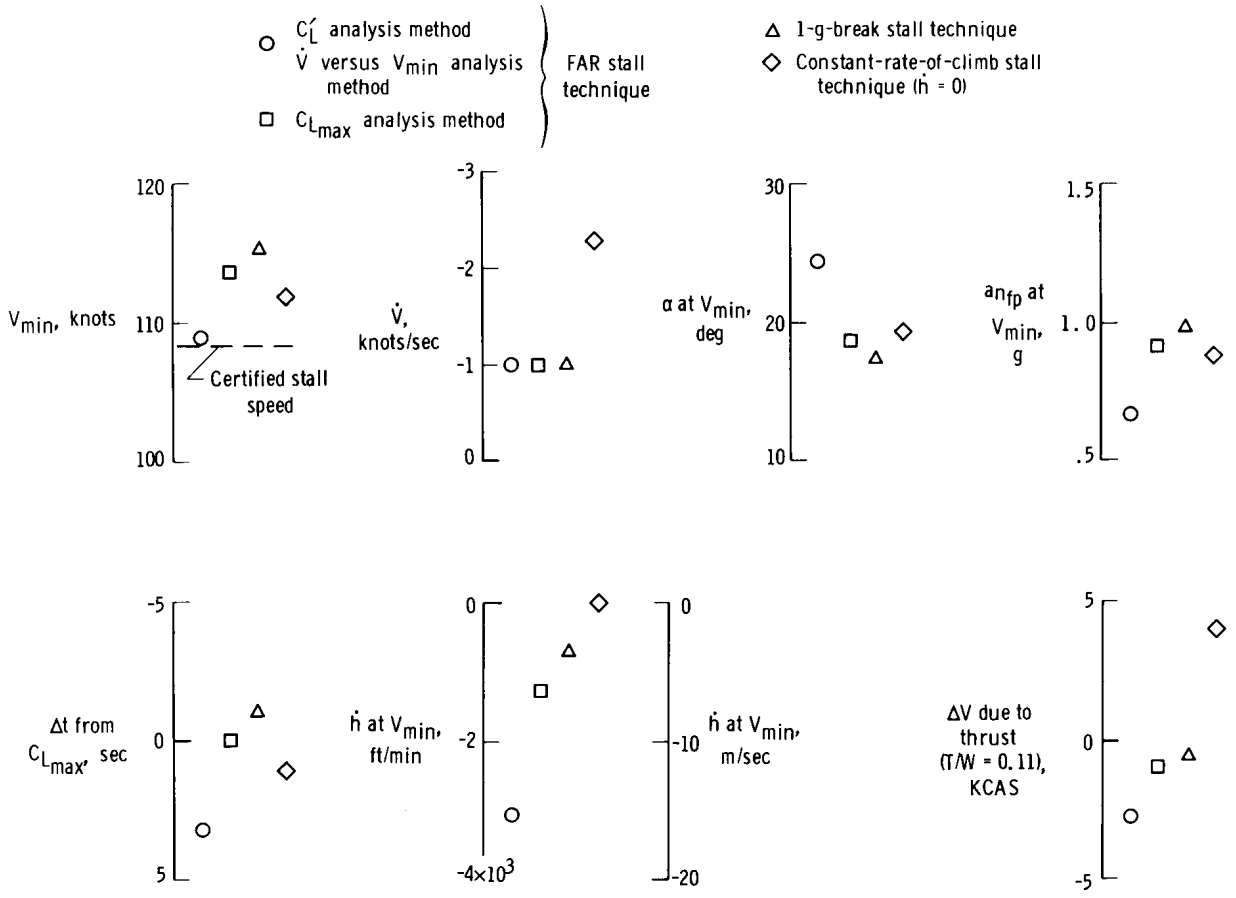


*(b) Comparison of eight parameters obtained at the minimum flying speed that each technique would define; $W_{corrected}$ = 165,000 lb (74,745 kg).*

*Figure 5. Concluded.*

A comparison of the minimum flying speeds $V_{min}$ established by each technique shows that the FAR technique yields the lowest and the 1-g-break technique yields the highest minimum velocity. The dashed line shows the handbook certified stall speed.

A comparison of the decelerations $\dot{V}$ at which the minimum flying speed would be specified shows that the zero-rate-of-climb speed is strongly affected by the deceleration of the maneuver (-2.3 knots/second), whereas, for the other techniques, the deceleration can be controlled somewhat or at least specified. The total dynamics of the maneuver are discussed in appendix B.

The plot of $\alpha$ at $V_{min}$ shows the angles of attack that would be achieved for each technique at the defined minimum flying speed. Although the FAR stall speed may not be directly related to angle of attack, it is of interest to compare the two quantities. The calculated $C_{L_{max}}$ occurred at an $\alpha$ of approximately 18°, whereas the 1-g break occurred when $\alpha$ was approximately 17°. The $\alpha$ at the $\dot{h}$-break was approximately 19°, with $\alpha$ equal to approximately 24° for the FAR-defined speed. These results would indicate that the angles of attack obtained from the 1-g-break technique and the $\dot{h}$-break technique are very similar to that obtained at $C_{L_{max}}$ and that the

angles of attack derived from the FAR techniques are nonconservative with respect to $\alpha$ at $C_{L_{max}}$.

A comparison of the flight-path normal-acceleration levels at the minimum speed $a_{n_{fp}}$ at $V_{min}$ shows the 1-g-break technique to be the most conservative, with the FAR technique the least conservative.

The plot of $\Delta t$ from $C_{L_{max}}$ compares the time difference from the point where $C_L$ actually maximizes to the point where $V_{min}$ would be determined. Of course, the $C_{L_{max}}$ technique has a zero time difference. The 1-g break actually takes place 1 second before $C_L$ maximizes, indicating that the $V_g$ would be conservative with respect to the speed at $C_{L_{max}}$. The zero-rate-of-climb speed occurs 1 second after $C_L$ maximizes, which indicates slight nonconservatism. The FAR speed falls approximately 3 seconds after $C_L$ maximizes and is the least conservative technique.

A comparison of the rates of climb at the minimum flying speed $\dot{h}$ at $V_{min}$ yielded by each technique shows that the 1-g-break speed has an associated $\dot{h}$ of -800 feet per minute (-4 meters per second), and the FAR-derived speed reaches an $\dot{h}$ of -3000 feet per minute (-15 meters per second). The $\dot{h}$ at $C_{L_{max}}$ is -1300 feet per minute (-6.5 meters per second).

The effects of thrust on the minimum flying speed derived by each technique are compared in the plot of $\Delta V$ due to thrust, in which $\Delta V$ is the velocity change produced by increasing the thrust-to-weight ratio from less than 0.02 to 0.11. The FAR-derived speed is lowered by 2.5 knots; the speed at $C_{L_{max}}$ is lowered by 1 knot; the 1-g-break speed is lowered by 0.5 knot; and the zero-rate-of-climb speed is raised by 4 knots.

One further comparison of the three basic techniques can be made by using reference 3 in conjunction with the present study. On the basis of data in reference 3, the present study, and some unpublished general-aviation data, it would appear that the 1-g-break and the constant-rate-of-climb techniques would be applicable to any type of aircraft configuration, whereas the FAR technique requires a well-defined maximum lift coefficient to yield optimum results.

## CONCLUDING REMARKS

Three techniques for determining the minimum flying speed for a large, subsonic jet transport in the landing configuration were investigated and compared. The techniques evaluated were the Federal Aviation Regulation (FAR) demonstration technique, the 1-g-break technique, and the constant-rate-of-climb technique. The program consisted of 7 pilot familiarization and 18 data-acquisition flights, during which approximately 175 stall maneuvers, most in the landing configuration, were performed.

The flight-path 1-g break was considered to be the best overall technique and the most conservative with respect to the maximum lift capability of the airplane. The dynamic effects of this maneuver on the minimum speed were the least of the three techniques tested and could be partially controlled by specifying the deceleration. Also, the minimum speed defined in this manner was not appreciably affected by thrust-to-weight ratios as high as one-half of the maximum capability of the test airplane at the test gross weight. However, the determination of the 1-g break was complicated by airplane buffeting.

The constant-rate-of-climb technique, when considered only at zero rate of climb for defining the minimum flying speed, was slightly nonconservative with respect to the maximum lift capability. In this instance, the zero-rate-of-climb break occurred approximately 1 second after maximum lift coefficient was reached. This effect was due to the dynamics of the maneuver, particularly, the deceleration. The deceleration, or time rate change of speed, approaching the stall was found to be more effective than thrust in producing a lower minimum airspeed at zero rate of climb for thrust levels up to one-half the maximum available thrust. This technique should be considered as an acceptable alternate for the 1-g-break technique.

The FAR Part 25 demonstration technique was analyzed by using two current analysis methods. Both yielded less conservative results than the 1-g-break or the constant-rate-of-climb techniques when compared with the conditions corresponding to maximum lift coefficient. At the stall speed defined by this technique, the sink rates were high, the normal-acceleration levels were low, and the angles of attack were 6° to 7° in excess of that obtained at the flight-determined maximum lift coefficient. The effect of thrust in this technique was to lower the minimum speed by approximately 2.5 knots. A third analysis method, the actual-maximum-lift-coefficient method, when modified and based on the actual maximum lift coefficient, would yield realistic results.

In applying the results of this study to other configurations, it would appear that the flight-path 1-g-break technique would yield realistic results on most wing planforms being used today as well as on the next generation of "jumbo" jets or supersonic transports. The constant-rate-of-climb technique appears to have the same general utility as the flight-path 1-g-break technique; however, the constant-rate-of-climb technique is strongly affected by the deceleration dynamics of the maneuver, and the deceleration is highly dependent on lift-to-drag ratio of the individual configurations at the higher angles of attack. The current FAR technique would be applicable only to those configurations having a well-defined maximum lift capability.

**Flight Research Center,**
**National Aeronautics and Space Administration,**
**Edwards, Calif., January 30, 1970.**

## APPENDIX A

## COMPARISON OF THE EFFECTS OF A FLIGHT-PATH ACCELEROMETER AND A BODY-AXIS ACCELEROMETER ON THE 1-g-BREAK STALL TECHNIQUE

The appendix of reference 3 derives the equations for the 1-g-stall minimum speed based on both flight-path and body-axis accelerometers. The equations are based on the following assumptions: quasi-steady-state conditions; two-degree-of-freedom performance problem; and negligible control effectiveness, moments, and transient effects (such as transient lift).

For the flight-path accelerometer the equation derived was

$$V_g = \left[\frac{2W}{\rho_o S C_{L_{max}}}\left(1 - \frac{T}{W}\sin\alpha^*\right)\right]^{1/2} \tag{A1}$$

For the body-axis accelerometer the expression was

$$V_g = \left[\frac{2W}{\rho_o S C_{L_{max}}}\left(\frac{1}{\cos\alpha^* + \frac{\sin\alpha^*}{(L/D)^*}}\right)\right]^{1/2} \tag{A2}$$

Further, assuming that the thrust-to-weight ratio is small (less than 0.02 for most of the flights) and can be neglected, the difference between the two equations is the term

$$\left(\frac{1}{\cos\alpha^* + \frac{\sin\alpha^*}{(L/D)^*}}\right)^{1/2} \tag{A3}$$

This term is evaluated for various values of $\alpha^*$ and $(L/D)^*$ in table A1. For example, if a particular configuration (a delta wing) has an $\alpha^*$ of 24°, an $(L/D)^*$ of 2, and a flight-path-accelerometer calibrated airspeed of 100 knots, the body-axis-accelerometer minimum airspeed would be approximately 94.6 knots.

TABLE A1.–VALUES OF EQUATION (A3) FOR VARIOUS VALUES OF $\alpha^*$ AND $(L/D)^*$

| $\alpha^*$, deg \ $(L/D)^*$ | 1 | 2 | 3 | 4 | 5 | 6 | 7 | 8 | 9 | 10 |
|---|---|---|---|---|---|---|---|---|---|---|
| 10 | 0.929 | 0.966 | 0.979 | 0.986 | 0.990 | 0.993 | 0.995 | 0.997 | 0.998 | 0.999 |
| 12 | .918 | .961 | .977 | .985 | .990 | .994 | .996 | .998 | .999 | 1.000 |
| 14 | .908 | .957 | .976 | .985 | .991 | .995 | .998 | 1.000 | 1.001 | 1.003 |
| 16 | .899 | .954 | .974 | .985 | .992 | .996 | 1.000 | 1.002 | 1.004 | 1.006 |
| 18 | .891 | .951 | .974 | .986 | .994 | .999 | 1.002 | 1.005 | 1.007 | 1.009 |
| 20 | .883 | .949 | .974 | .988 | .996 | 1.001 | 1.005 | 1.009 | 1.011 | 1.013 |
| 22 | .876 | .947 | .975 | .990 | .999 | 1.005 | 1.010 | 1.013 | 1.016 | 1.019 |
| 24 | .870 | .946 | .976 | .992 | 1.003 | 1.009 | 1.014 | 1.018 | 1.021 | 1.024 |
| 26 | .865 | .946 | .978 | .996 | 1.007 | 1.014 | 1.020 | 1.024 | 1.027 | 1.030 |
| 28 | .860 | .946 | .981 | 1.000 | 1.012 | 1.020 | 1.026 | 1.031 | 1.034 | 1.037 |
| 30 | .856 | .947 | .984 | 1.005 | 1.017 | 1.026 | 1.033 | 1.038 | 1.042 | 1.045 |

For the test airplane, the steady-state $\alpha^*$ was predicted to be 12° to 13° and the $(L/D)^*$ was predicted to be 7.5. This would imply a spread of less than 0.4 knot between the two speeds, assuming that they are affected similarly by the dynamics of the maneuvers. However, in flight, as figure 5(b) shows, the stall angle of attack approached 18° and the $(L/D)^*$ was between 6 and 7. Referring to table A1, the difference between the two airspeeds would be less than 0.2 knot.

A series of stall maneuvers (18 with a flight-path accelerometer and 11 with a body-axis accelerometer) was performed to compare the two systems. The results of these tests are shown in figure 6 along with a calculated value of $V_g$ obtained by

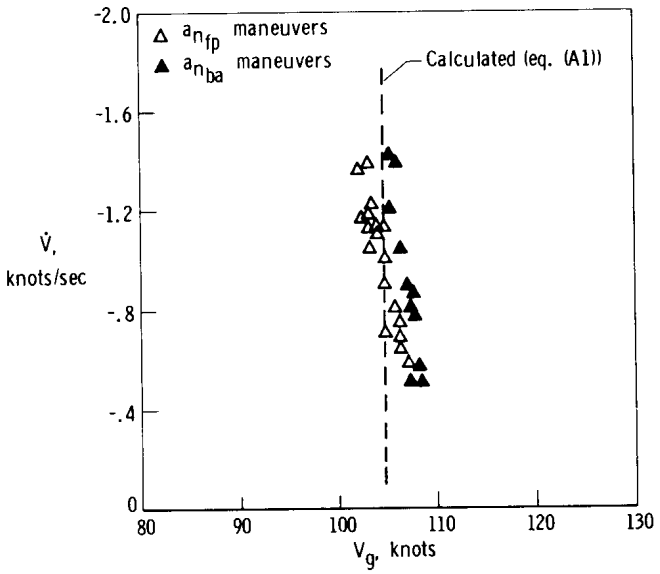


*Figure 6. Comparison of the effects of flight-path acceleration and body-axis acceleration on data obtained during the 1-g-break stall maneuvers performed in the landing configuration. $W_{corrected}$ = 140,000 lb (63,500 kg); center of gravity = 22.6 percent to 24.9 percent $\bar{c}$; h = 13,600 ft (4148 m) to 18,200 ft (5547 m).*

using the predicted value of $C_{L_{max}}$. As shown, the maneuvers in which the body-axis acceleration was used yield generally higher speeds than the maneuvers in which the flight-path acceleration was used. However, at the lower $\dot{V}$, the difference between the speeds approaches the value predicted by table A1. These differences or divergences, or both, are probably due primarily to the methods used to analyze the data. Since the two accelerometers have different reference axes systems—the body axis and the stability axis—the absolute values of their outputs need not be the same. In the 29 maneuvers used in figure 6, the data from the body-axis accelerometer were lower than those from the flight-path accelerometer. As shown in the adjacent sketch, since the body-axis accelerometer values were lower, the point where the g-break was chosen (0.97 g) occurred earlier than it would have with the flight-path system. Although $\Delta t$ was fairly constant, the calibrated airspeed varied, because, as $\dot{V}$ increased, $\dot{V}\Delta t$ also increased, resulting in the divergence in $V_g$ shown in figure 6.

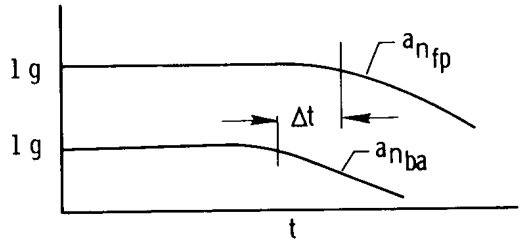

## APPENDIX B

## EFFECTS OF $\dot{\alpha}$ ON MAXIMUM LIFT COEFFICIENT DURING A 1-g-BREAK STALL MANEUVER

In this paper no distinction has been made between deceleration dynamics and rotational dynamics; however, in this appendix, transient effects are separated into the two categories. The deceleration dynamics are primarily dependent on the derivative $C_{L_u}$ and inertial factors. The rotational dynamics are primarily dependent on the derivatives $C_{L_{\dot{\alpha}}}$ and $C_{L_q}$. The pitching angular velocity was generally of the same order as $\dot{\alpha}$, and its effects were not separated from the $C_{L_{\dot{\alpha}}}$ effects.

During the performance of the normal stall maneuvers in the study, $\dot{\alpha}$ was found to vary generally with $\dot{V}$; that is, the higher $\dot{\alpha}$ was generally associated with the higher $\dot{V}$ with normal use of the pilot's controls. However, when the pilot made other than normal control inputs, i.e., very large or very small, just prior to the stall, relatively large variations in $\dot{\alpha}$ and $C_{L_{max}}$ were obtained.

From 27 heavy-gross-weight, 1-g-break stall maneuvers a $C_{L_{max}}$ was calculated, and $\dot{V}$ and $\dot{\alpha}$ were measured. The results are shown in figure 7. The $\dot{\alpha}$ data were assembled into three groups, since effects of the $\dot{\alpha}$ and $\dot{V}$ could not be separated more clearly. For the maneuvers used in this paper, a limit of 2.5 deg/sec was used for $\dot{\alpha}$, and maneuvers in which $\dot{\alpha}$ exceeded 2.5 deg/sec were disregarded. If the half-solid symbols in figure 7 were disregarded, the remaining data would yield the

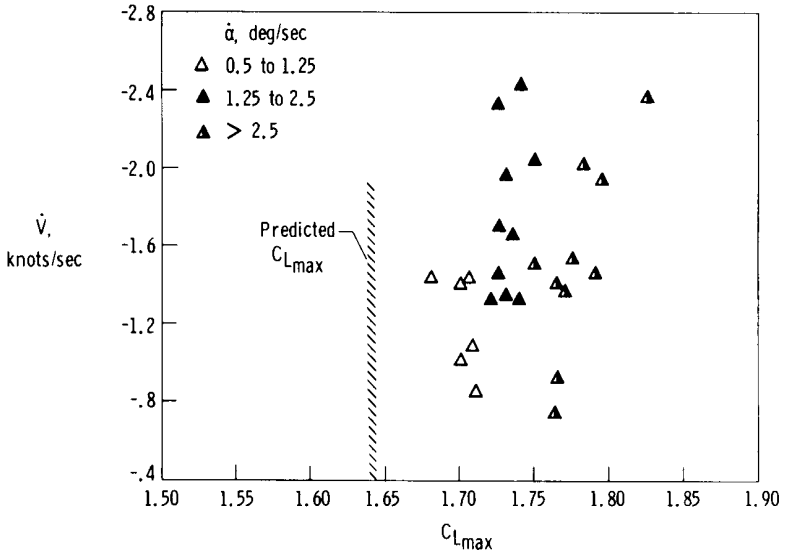


*Figure 7. Effects of $\dot{\alpha}$ and $\dot{V}$ on $C_{L_{max}}$ for the 1-g-break stall maneuvers. W = 180,000 lb (81,540 kg) to 204,000 lb (92,412 kg); center of gravity = 23.1 percent to 26.2 percent $\bar{c}$; landing configuration.*

expected trend of $\dot{V}$ versus $C_{L_{max}}$. Note that all the flight points are above the predicted $C_{L_{max}}$.

The information in figure 7 implies that, regardless of the deceleration (and, more generally, of the type of stall maneuver performed), if the pilot makes the proper control inputs to obtain high $\dot{\alpha}$ values at the proper time, for example, just prior to 1-g break, the minimum speed derived could be reduced by 2 or 3 knots. The speed derived in this manner would be, naturally, from a highly transient condition and not realistic for a minimum flying speed.

## REFERENCES


1. Anon.: Federal Aviation Regulations. Part 25—Airworthiness Standards: Transport Category Airplanes. FAA, Oct. 6, 1967.

2. Fischel, Jack; Butchart, Stanley P.; Robinson, Glenn H.; and Tremant, Robert A.: Flight Studies of Problems Pertinent to Low-Speed Operation of Jet Transports. NASA MEMO 3-1-59H, 1959.

3. Powers, Bruce G.; and Matheny, Neil W.: Flight Evaluation of Three Techniques of Demonstrating the Minimum Flying Speed of a Delta-Wing Airplane. NASA TN D-2337, 1964.

4. Cheney, H. K.: SST Flight Test Requirements for Certification of Take-Off/Landing Performance. Soc. Exp. Test Pilots Quarterly Review, vol. V, no. 4, Sept. 1961, pp. 175-199.

5. Clark, Harry F.; and Marthinsen, Harold F.: Committee No. 3 Operational Noise Abatement Procedures Designed To Limit the Amount of Disturbance Caused by Aircraft Taking Off, In Flight, or Landing. Paper presented at International Conference on the Reduction of Noise and Disturbance Caused by Civil Aircraft (London, Eng.) Nov. 1966.

6. Poole, J.: Some Recent Flight Testing Experience at A. & A.E.E. Boscombe Down. AIAA Paper No. 64-783, 1965.

7. Tymczyszyn, Joseph J.; and Spiess, Paul C.: The Effects of Supersonic Transport Flight Characteristics on Performance Requirements. SAE paper 674 D, 1963.

8. Innis, R. C.: Factors Limiting the Landing Approach Speed of Airplanes From the Viewpoint of a Pilot. AGARD Rep. 358, 1961.

9. Wimpenny, J. C.: Low-Speed Stalling Characteristics. AGARD Rep. 356, 1961.

10. Anon.: Flying Qualities of Piloted Airplanes. Military Specification MIL-F-008785A(USAF), Oct. 31, 1968.

11. Herrington, Russel M.; Shoemacher, Paul E.; Bartlett, Eugene P.; and Dunlap, Everett W.: Flight Test Engineering Handbook. Tech. Rep. No. 6273, Air Force Flight Test Center, May 1951 (rev. Jan. 1966).

12. Yaggy, Paul F.: A Method for Predicting the Upwash Angles Induced at the Propeller Plane of a Combination of Bodies With an Unswept Wing. NACA TN 2528, 1951.